Personal Account

THE CHEMICAL RECORD

doi.org/10.1002/tcr.202500077
tcr.wiley-vch.de

Synthesis and Transformations of Bioactive Scaffolds via Modified Mannich and *aza*-Friedel–Crafts Reactions

Dóra Hegedűs, Nikoletta Szemerédi, Gabriella Spengler, and István Szatmári*

Abstract: This account summarizes the synthesis of bifunctional glycine-type precursors substituted with 2- and 1-naphthol. The stabilization of precursors via partially aromatic *ortho*-quinone methide intermediate is tested with different cyclic imines in [4 + 2] cycloaddition. 8-Hydroxyquinoline is a biologically active moiety considered as a formal 1-naphthol analog, hence the behavior of the scaffold in Mannich reaction is examined. The possibility of transformation of glycine derivatives substituted with 2- and 1-naphthol as well as the formed Mannich base consisting 5-chloro-8-hydroxyquinoline skeleton to give diarylmethane derivatives with indole and 7-azaindole are studied. A series of cyclic amines coupled with indole and azaindole derivatives has been systematically designed and their biological examination is achieved. To have a preliminary overview about the structure–activity relationship, the antibacterial and anticancer activity of synthesized compounds by preliminary biological screening systems is tested.

Keywords: [4 + 2] cycloaddition, anticancer activity, efflux pumps, modified Mannich reaction, *ortho*-quinone methides

1. Introduction

The Mannich reaction is a widely used three-component reaction in organic chemistry for C—C and C—N bond formation.[1–5] A special variation of this latter reaction (modified Mannich reaction: *m*MR) uses benzaldehyde rather than formaldehyde, ammonia instead of secondary amine and replacing the C—H acid by an electron-rich aromatic compound, such as 1- or 2-naphthol[6] or nitrogencontaining naphthol analogs leading to chelating compounds with improved antiproliferative activity.[7]

Our research group reported an unexpected transformation between 1-*α*-aminobenzyl-2-naphthol and 3,4-dihydroisoquinoline enabled the synthesis of naphth[1,2-*e*][1,3]oxazino[2,3-*a*] isoquinolines under microwave (MW) irradiation.[8] As a next step, the reaction was extended to 2-aminoalkyl-1-naphthols[9] and other C═N dienophiles (cyclic imines) allowing the synthesis of new naphthoxazino-isoquinoline, -benzazepine, and -thienopyridine derivatives.[10] The synthesis of new nonracemic naphth[1,3] oxazino[3,2-*a*]quinoxalinones starting from enantiomeric (4*aS*, 8*aS*)-4*a*,5,6,7,8,8*a*-hexahydro-2-quinoxalinone and 1-aminoalkyl-2-naphthols or 2-aminoalkyl-1-naphthols has already been achieved.[11,12] As a result of a recent work, the reactivity of highly functionalized aminonaphthol[13] or aminophenanthrol derivatives[14] with different cyclic imines was also tested in [4 + 2] cycloaddition. Our research group examined the formation and transformation of aromatic *ortho*-quinone methides (*o*-QM) via [4 + 2] cycloaddition.[12] To the best of our knowledge, the stabilization of partially aromatic *o*-QMs with cyclic imines has not been

D. Hegedűs, I. Szatmári
Institute of Pharmaceutical Chemistry
University of Szeged
Eötvös u. 6, H-6720 Szeged, Hungary
E-mail: szatmari.istvan@szte.hu
N. Szemerédi, G. Spengler
Department of Medical Microbiology
Albert Szent-Györgyi Health Center and Albert Szent-Györgyi Medical School
University of Szeged
Semmelweis utca 6, 6725 Szeged, Hungary
I. Szatmári
HUN-REN–SZTE Stereochemistry Research Group
University of Szeged
Eötvös u. 6, H-6720 Szeged, Hungary

studied. Consequently, our first aim was to prepare bifunctional glycine-type precursors substituted with 2- and 1-naphthol. The stabilization of precursors via partially aromatic *ortho*-quinone methide intermediate formed in the retro-Mannich reaction was tested with different cyclic imines in [4 + 2] cycloaddition.

8-Hydroxyquinoline (8-OHQ) is a biologically active moiety[7] considered as a potential 1-naphthol analog. 8-OHQ can be interpreted as potential substrate of the Mannich reaction, which is a privileged structure in many biologically active compounds and several marketed drugs[15] used for the treatment of infectious diseases, neuropathies, and cancers. Taking into consideration that the diverse biological activities of 8-OHQ derivatives can be fine-tuned by modification of the substitution pattern of the scaffold,[16–19] we proposed to examine the behavior of 5-Cl-8-HQ in the modified Mannich reaction by using ethyl glyoxylate as aldehyde component.

Recently, the formation of triarylmethane derivatives consisting of indole known as potent biological moiety and 2-naphthol[20–22] or the ethyl ester of kynurenic acid[23] has been described. As a further aim of the research, testing the reactivity of glycine derivatives substituted with 2- and 1-naphthol with indole and 7-azaindole was also planned. We targeted additionally to study the possibilitiy of transformation of the formed Mannich base consisting 5-Cl-8-HQ skeleton to give diarylmethane derivatives with indole and 7-azaindole as well as the effect of the aldehyde component and the amine part of the Mannich base on the synthetic pathway.

As a special *m*MR, the modified *aza*-Friedel–Crafts reaction by direct coupling of different cyclic imines and indole derivatives as electron-rich aromatic compounds have been studied.[24–26] To investigate the scope and limitations of the reaction and examine the effect of structural modifications were part of our experiments, which can offer possibilities for having a preliminary overview about the structure–activity relationship for C-3-coupled indole and azaindole derivatives. Therefore, we focused our efforts on resynthesizing selected compounds (3-isoquinolyl-, 3-thieno[3,2-*c*]pyridyl-, 3-*β*-carbolinyl-, and 3-benz[*c*]azepinyl-indole and -azaindole derivatives) as well as preparing new derivatives starting from 6,7-dimethoxy-3,4-dihydroisoquinoline, (4*aR*,8*aR*)-4*a*,5,6,7,8,8*a*-hexahydroquinoxalin-2(1*H*)-one and 7-azaindole.

Additionally, our aim was to have a preliminary overview about the structure–activity relationship, we targeted to test the antibacterial and anticancer activity of synthesized compounds by preliminary biological screening systems.

1.1. Transformations of 2-, and 1-Naphthol Skeleton via Application of Ethyl Glyoxilate or Glyoxylic Acid

Chasset and co-workers reported the transformation of 2-naphthol (**1**) and ethyl glyoxalate (**2**), accordingly using titanium chloride ($TiCl_4$) two reaction pathways were proposed resulted in preparation of intermediate ethyl 2-hydroxy-2-(2-hydroxynaphthalen-1-yl)acetate (**3**) and ethyl 2-ethoxy-2-(2-hydroxynaphthalen-1-yl)acetate (**5**) (**Scheme 1**). The invention provided new antiviral agents, especially anti-retroviral agents, and more particularly anti-HIV compounds.[27]

The preparation of a diverse range of pharmaceutically important pyran annulated heterocycle **6** in the presence of highly reusable ionexchange polystyrene resin Amberlyst A21 as a surrogate solid base catalyst was achieved (**Scheme 2**).[28] Seidel and co-workers published a redox-neutral strategy that enables the simultaneous *α*,*β*-difunctionalization of amines via transient enamines. The synthesis of polycyclic *N,O*-acetals from simple 1-(aminomethyl)-*β*-naphthols and 2-(aminomethyl)-phenols was achieved (Scheme 2).[29]

Zhou and co-workers reported novel *N*-arylnaphthofuranone imine analogs **8a-e** by using aryl aromatic amines, 2-naphthol analogs, and glyoxylates in the presence of oxygen oxidation.[30] The high adaptability to functional groups (such as alkyl, alkoxy, aryl, halogen, nitro, and trifluoromethyl), simple reaction conditions, easy separation of target product, and high yield can be referred as advantages of the method (**Table 1**).

Cimarelli and co-workers described a novel synthesis of enantiomerically pure arylglycinates **9, 10** via the spontaneous reaction between either phenol or naphthol derivatives and enantiopure glyoxylate imine in the absence of an acid catalyst (**Scheme 3**). Diastereoisomerically pure aryl glycinates were obtained via flash chromatographic separation of the crude reaction mixture. The diastereomeric ratio of **9a**:**9b** was found to be 82:18, **10a**:**10b** was found to be 77:23. Optical rotations were measured in the case of compounds **9a,b** and **10a**.[31] Additionally, the research group found that the free naphthol

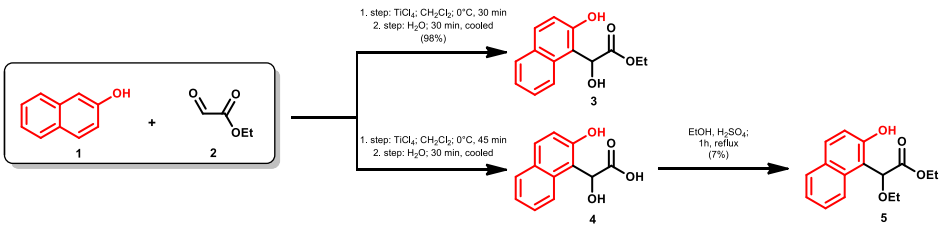

Scheme 1. Titanium chloride mediated synthesis starting from compounds **1** and **2**.

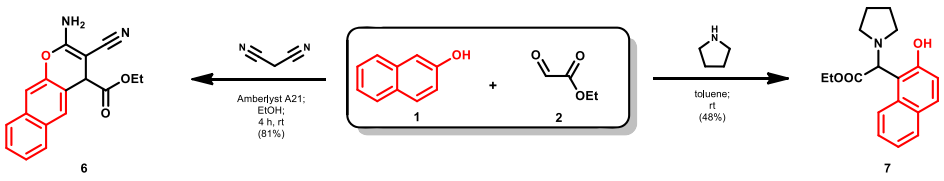

Scheme 2. Transformations of 2-naphthol (**1**) and ethyl glyoxylate (**2**) with malononitrile as well as pyrrolidine.

Table 1. Synthesis of *N*-arylnaphthofuranone imine analogs.

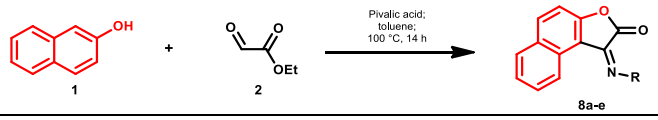

Entry	Reactant (amines)	Product	Yields [%]	Lit.
1.	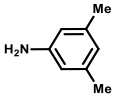	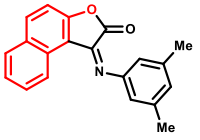	94	30
2.	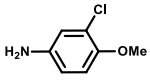	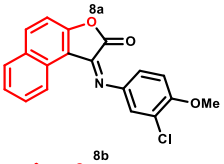	85	30
3.	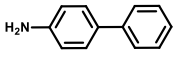	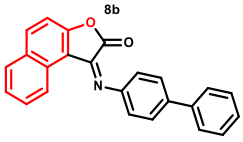	88	30
4.	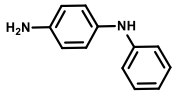	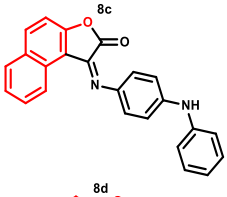	90	30
5.		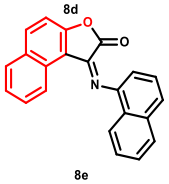	88	30

OH moiety probably promoted a cyclic transition state, activating the imino group in situ via intermolecular hydrogen bonding, and promoting the reaction in the absence of an acid catalyst.

In the case of the synthesis of 2-hydroxy-2-(6-hydroxynaphthalen-2-yl)acetic acid (**12**), the method presented in the literature involved the reaction starting from 2-napthol (**1**), glyoxylic acid monohydrate (**11**), KOH under cooling (Method A) (**Scheme 4**).[32] In addition, substituted mandelic acids were prepared by reacting a mixture of NaOH solution, corresponding substituted phenols and glyoxalic acid (**11**) in the presence of a phase transfer catalyst (cetyl trimethyl ammonium bromide—CTAB) (Method B) and transformed to 2-(1,3-dioxo-2,3-dihydro-1H-2-isoindolyl) ethyl 2-hydroxy-2-(substituted phenyl) acetates by using *N*-(2-hydroxy ethyl) phthalimide.[33] By a base-catalyzed condensation of 2-naphthol (**1**) with glyoxylic acid (**11**), the synthesis of racemic α-hydroxy-α-(2-hydroxy-1-naphthyl)acetic (**4**) acid

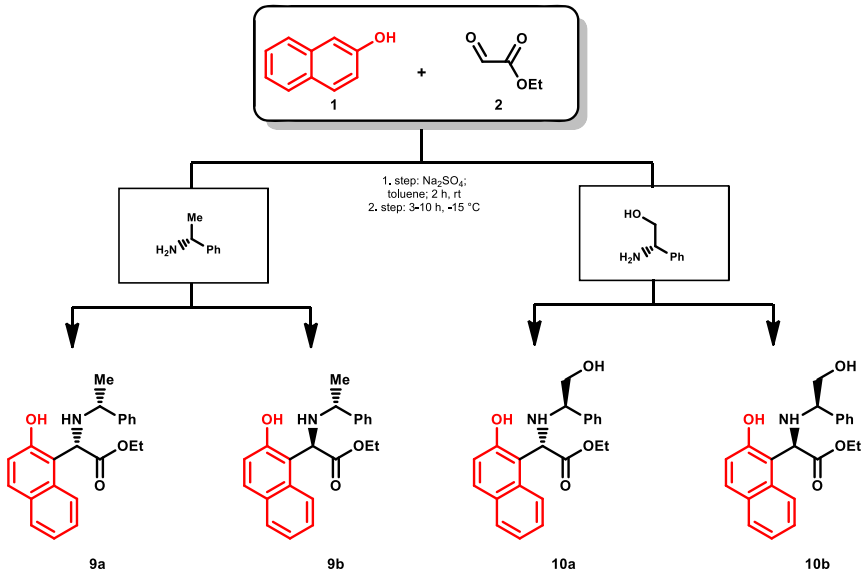

Scheme 3. Preparation of enantiomerically pure arylglycinates.

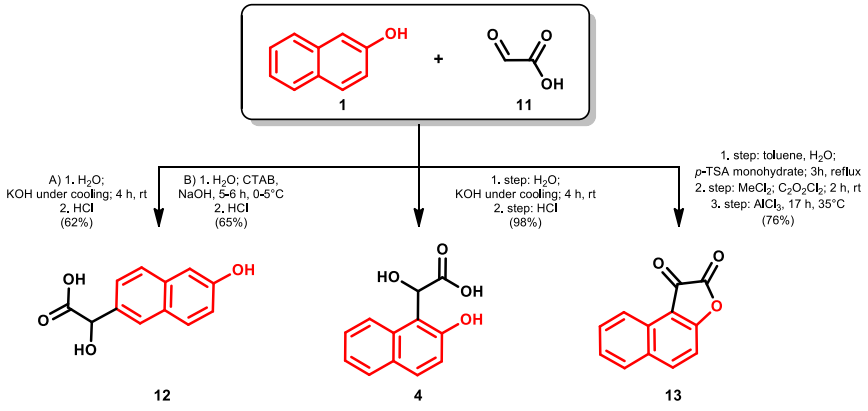

Scheme 4. Methods for reacting 2-naphthol (**1**) with glyoxylic acid (**11**).

was achieved.[34] The synthesis of benzofuran-2-ones **13** which in particular possess good solubilities in addition to giving good performance properties such as heat and light fastness and strong, transparent, and bright colorations were described by a patent (Scheme 4).[35]

The reaction between 2-naphthol (**1**) and glyoxylic acid (**11**) in the presence of benzylamine resulted in the formation of *N*-benzyl-(2-hydroxy-1-naphthyl)glycine (**14a**) (**Scheme 5**).[36] Fessner and co-workers established the amido-alkylation of electron-rich arene **1** with phenylacetamide and glyoxylic acid (**11**) resulted in *N*-phenylacetylated arylglycine **14b** that are suited for immediate enzymatic resolution by penicillin G acylase.[37] One-step synthesis of *N*-heteroaryl α-naphthylglycines **14c-g** was carried out by the reaction of 2-naphthol (**1**), aqueous glyoxalic acid (**11**) with heteroaryl amines (2-aminopyridine, 3-aminopyridine, 3-amino-2-chloropyridine, 2-aminopyrazine, and 2-aminopyrimidine) in water at ambient temperature and under reflux conditions.[38]

Recently, an efficient one-pot synthesis of hydroxynaphthyl-substituted glycine derivatives **15, 16** from 2-naphthol (**1**), glyoxylic acid (**11**), and benzyl carbamate in the presence of *p*-TSA via a modified Mannich reaction is described.[39] As next steps, after removal of the benzyloxycarbonyl group by catalytic (Pd/C) hydrogenation, hydrolysis (5% aq HCl) was carried out. Csütörtöki et al. extended the synthetic method by testing MeOH as well as EtOH as solvent. To test other carbamates, in the reaction of 2-naphthol (**1**) with glyoxylic acid (**11**) in the presence of *p*-TSA using MeOH as solvent, *tert*-butoxy

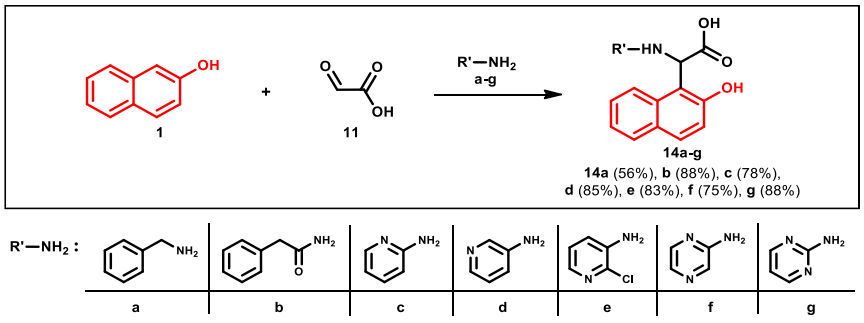

Scheme 5. Synthesis of *N*-aryl α-naphthylglycines starting from derivatives **1** and **11** in the presence of various amines.

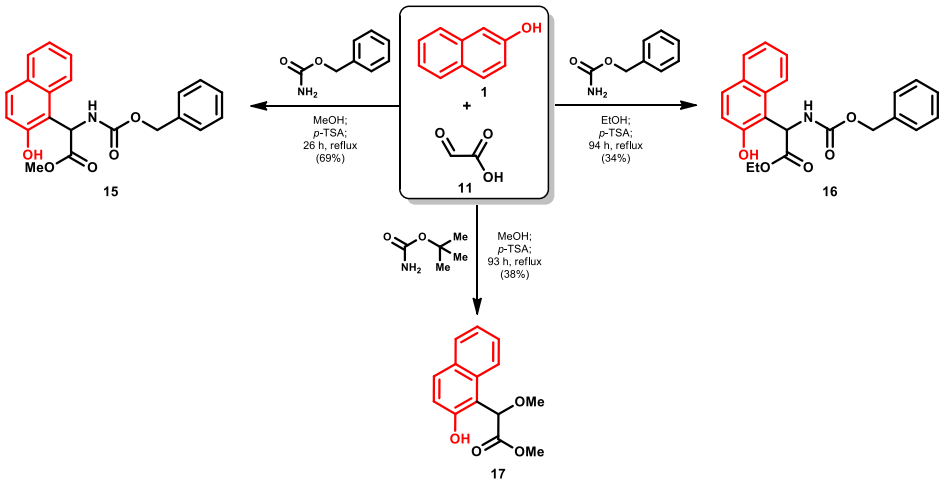

Scheme 6. Preparation of hydroxynaphthyl-substituted glycine derivatives by testing different carbamates.

carbamate (NH_2Boc) was applied (**Scheme 6**). Developing an analytical protocol for the enantioseparation of the synthesized racemic aminoesters was part of the study, the absolute configurations were determined by CD analysis supported by TDDFT CD calculations.

Palmieri and co-workers reported the spontaneous reaction between either naphthol or phenol derivatives and ethyl glyoxylate imines, in toluene at −15 °C, without the use of an acid catalyst, which led to arylglicinate **19** with moderate to high yields obtained after a few hours (**Scheme 7**). A variety of substituted phenol or naphthol glycinates were obtained in good yields and high diastereoselectivities. Diastereoisomerically pure aryl glycinates were obtained via flash chromatographic separation of the crude reaction mixture. The diastereomeric ratio of **19a**:**19b** was found to be 81:19. Optical rotation was measured in the case of compound **19a**.[31] The synthetic method starting from 2-naphthol (**1**) was presented previously in this chapter. The reaction of α-keto esters with phenols in the presence of a Lewis acid (mainly chlorides of metals in high oxidation state) provided in high yields (*o*-hydroxyaryl)-glycolic acid derivative **20** (Scheme 7).[40]

As a result of a previous research, amino acid derivatives are generated by a scandium triflate-catalyzed three-component reaction of phenols, glyoxylates, and amines. The three-component/one-pot reaction starting from 1-naphthol (**18**), ethyl glyoxylate (**2**), and 4-fluoroaniline afforded the corresponding product **21** (**Scheme 8**). The applied $Sc(OTf)_3$ could be recovered and reused. In the presence of Me_3SiCl, the yield of the product was improved considerably.[41]

The method applied by Rani et al. afforded the formation of 2-hydroxy-2-(5-hydroxynaphthalen-2-yl)acetic acid (**22**) in water with the aid of KOH under cooling in order to synthesize new hydroxy-(substituted-naphthalen-1-yl)-acetic acid 2-(1,3-dioxo-1,3-dihydro-isoindol-2-yl)-ethyl esters.[32] An invention described the preparation of 3-oxo-1-naphthofuranone (**23**) and the application as colorants for organic materials, especially organic materials of high or low molecular weight (**Scheme 9**).[35] In the case of both synthetic pathways for the

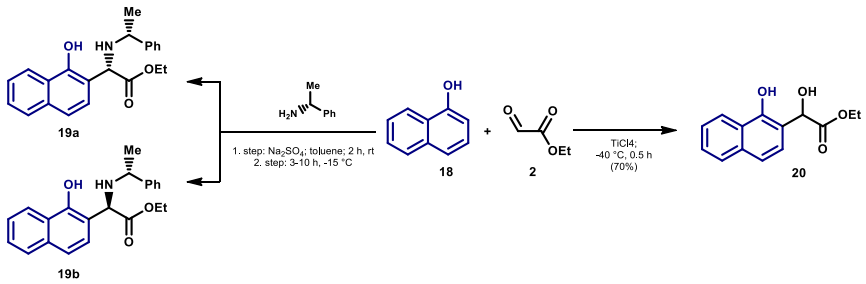

Scheme 7. Transformations of 1-naphthol (**18**) with ethyl glyoxylate (**2**) without the use of an acid catalyst or in the presence of a Lewis acid.

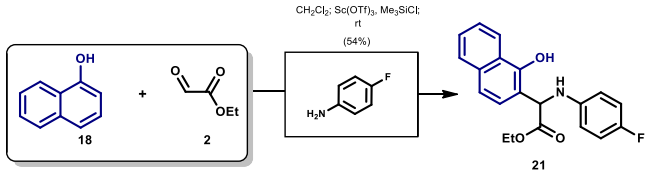

Scheme 8. Reacting 1-naphthol (**18**) with ethyl glyoxylate (**2**) in the presence of 4-fluoroaniline.

preparation of corresponding compounds either from 2-naphthol were subjected in previously in this chapter.

Previously, the one-pot synthesis of hydroxynaphthyl-substituted α-amino acid derivatives **15-17** starting from 2-naphthol (**1**), glyoxylic acid (**11**), and benzyl carbamate or *tert*-butoxy carbamate in the presence of *p*-TSA via a modified Mannich reaction was presented previously in this chapter. (Scheme 6). Next, to study the applicability of the reaction, the optimized reaction conditions were extended to 1-naphthol (**18**) as substrate (**Scheme 10**).[39]

1.2. Synthetic Method Starting from 8-Hydroxyquinoline as 1-Naphthol Analog and Ethyl Glyoxylate

A review of the scientific literature identified 8- hydroxyquinoline derivatives possessing multidrug-resistance reversing activity with improved selectivity and increased cytotoxicity towards multidrug-resistant cancer cells. In favor to form ethyl 2-(5-chloro-8-hydroxyquinolin-7-yl)-2-{[(2-fluorophenyl)methyl]amino}acetate (**28**), 5-chloro-8-hydroxyquinoline (**27**) considered as 1-naphthol analogue was reacted with 2-fluorobenzylamine and ethyl glyoxylate (**2**) in ethanol (**Scheme 11**).[42]

1.3. Transformations of Indole Skeleton

1.3.1. Synthetic Methods Starting from Indole and Ethyl Glyoxylate

Indole and imidazo[1,2-*a*]pyridine are known as important structural units found in many natural products, pharmaceuticals, and agrochemicals.[43] Regarding functionalization reactions, hydroxyalkylation at the C3-position of indole and imidazo[1,2-*a*]pyridine is accomplished by (*i*) Friedel–Crafts acylation/Vilsmeier−Haack formylation followed by reduction, and (*ii*) Friedel–Crafts hydroxyalkylation in the presence of acids including reaction with excess formalin in acetic acid. Furthermore, various synthetic protocols for Friedel–Crafts hydroxyalkylation to heterocycle ethyl-2-hydroxy-2-(1*H*-indol-3-yl)acetate (**30**) were reported. Among them, zinc triflate,[44] magnesium iodide,[45] scandium triflate,[46] *N,N*-dioxide,[46] titanium isopropoxide,[47] (-)-binol[47] were shown to be efficient catalysts for certain reactions. For the synthesis of compound **31**, besides the reaction of indole (**29**) with ethyl glyoxylate (**2**), iodine and sodium thiosulfate;[48] *N*-phenyl-*N*-2-piridinurea;[49] 1*H*-benzimidazolium,3,3′-(1,3-phenylene)bis[2-iodo-1-methyl-, 1,1,1 trifluoromethanesulfonate (1:2);[50] sodium dodecyl sulfate and ytterbium triflate;[51] triethylborane;[52] indion 225;[53] carbon tetrabromide, benzenesulfonic acid, sodium triphenylphosphine-*m*-sulfonate (TPPMS)—CBr_4 1:1 molar ratio complex;[54] silica, sodium iodide, cerium trichloride[55] were applied as reagents or catalyst. Soueidan et al. examined the reaction of ethyl

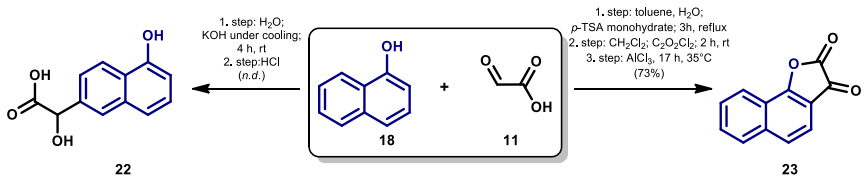

Scheme 9. Synthesis of 2-hydroxy-2-(5-hydroxynaphthalen-2-yl)acetic acid (**22**) and 3-oxo-1-naphthofuranone (**23**).

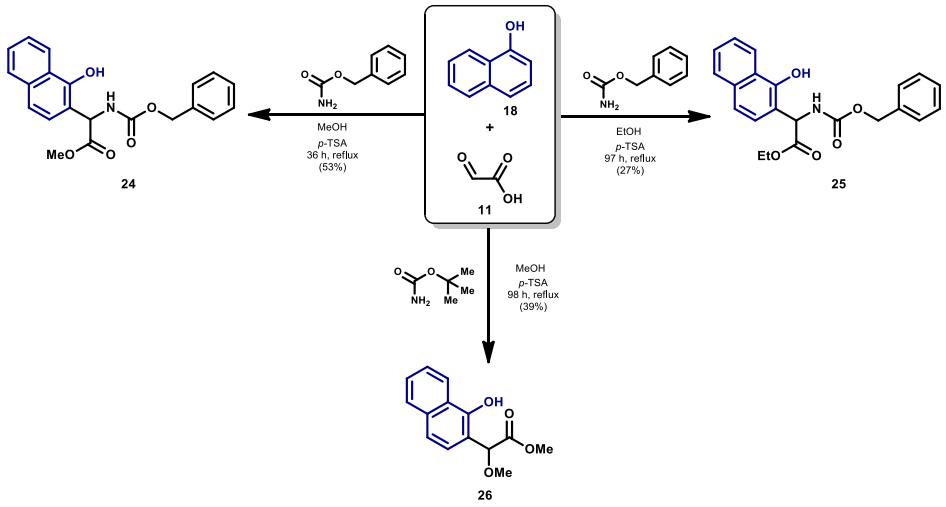

Scheme 10. Preparation of hydroxynaphthyl-substituted α-amino acid derivatives by testing different carbamates extended to 1-naphthol (**18**) as substrate.

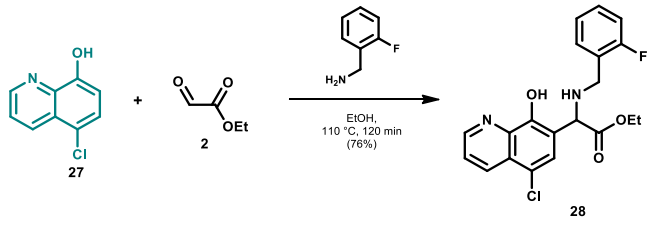

Scheme 11. Reaction starting from 5-chloro-8-hydroxyquinoline (**27**) as 1-naphthol analogue with ethyl glyoxylate (**2**).

glyoxylate (**2**) with indole (**29**) as aromatic compound in the presence of 10 mol% samarium diiodide. As result, the desired α-hydroxy-ester **30** (38%) and product **31** (22%) identified as arising from a double Friedel–Crafts reaction with dehydration.[56] The nickel-catalyzed dehydrogenative–decarboxylative coupling of indole (**29**) with ethyl 2-oxoacetate enabled the generation of 3-formylindole (**32**).[57] Furthermore, various indole hemiaminals **33** were prepared by organocatalyzed indole *N*-1 nucleophilic addition of α-oxoaldehydes.[58] The catalytic enantioselective Friedel–Crafts alkylation of indole with ethyl glyoxylate in 1,1,1,3,3-pentafluorobutane in the presence of fluorous cinchona alkaloid catalysts was achieved and resulted is products **30a** and **30b**.[59] Deng and co-workers showed that the asymmetric Friedel–Crafts alkylation catalyzed by bifunctional cinchona alkaloids led to the same products.[60] The transformations are summarized in **Scheme 12**.

In another study, catalyst-free three-component reaction of ethyl glyoxylate (**2**), a 1,3-dicarbonyl compound, and indole (**29**) as nucleophile was developed by using water as the solvent, which produced 1,4-ketoester **34**.[61] Li et al. developed a 1,1,1,3,3,3-hexafluoro-2-propanol-promoted de novo synthesis

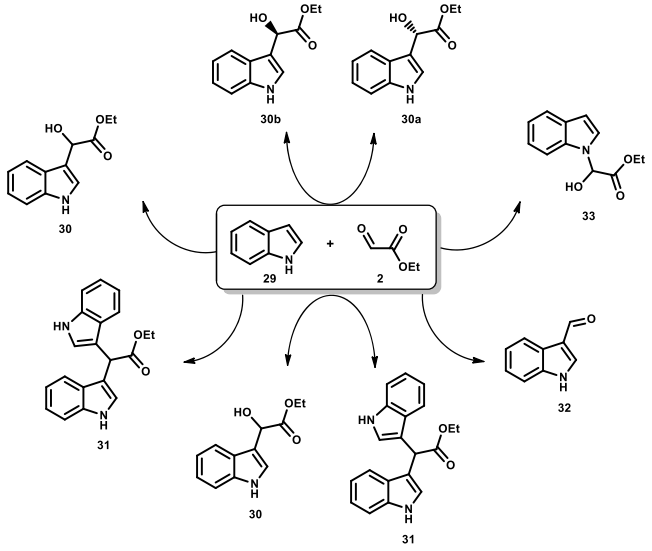

Scheme 12. Various synthetic protocols for transformation of indole (**29**) with ethyl glyoxylate (**2**).

of nonnatural α-arylated amino ester **35** from morpholine, ethyl glyoxylate (**2**), and indole (**29**) as electron-rich arene (**Scheme 13**).[62]

Desimoni and co-workers published the multi-component Friedel–Crafts alkylation reaction between indole (**29**), ethyl glyoxylate (**2**) and anilines, the expected ethyl 2-(arylamino)-2-(1*H*-indol-3-yl)acetates were formed (**Table 2**, entries 4-5, 7, 12-14, 17). The reactions between starting compounds with scandium triflate (5 mol%) in dichloromethane applying different reaction conditions (temperature, time) were investigated.[63] Kang et al. studied the chiral phosphoric acid-catalyzed

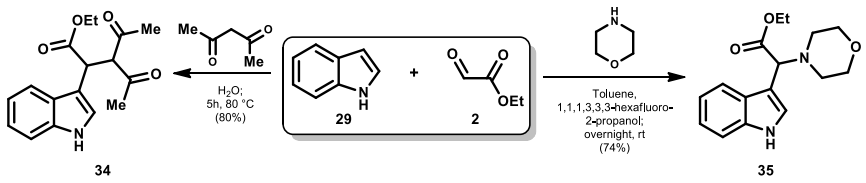

Scheme 13. Preparation of derivatives **34** and **35** by using 1,3-dicarbonyl compound and morpholine as applied reactants.

Table 2. Synthesis of 3-indolylglycine derivatives.

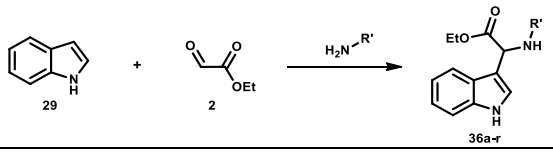

Entry	Reactant (amine)	Product	Reaction conditions				Yields [%]	Lit.
			Reagents	Catalyst	Solvent	T [°C], t [h]		
1		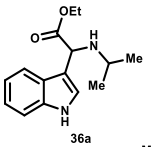 36a	$MgSO_4$	–	Toluene	rt, 72	33	68
2	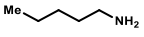	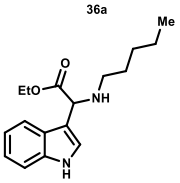 36b	$MgSO_4$	–	Toluene	rt, 72	49	68
3		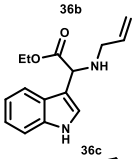 36c	–	–	–	rt, 1	61	69
4		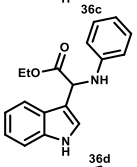 36d	–	–	CH_2Cl_2	rt, 20	85	63
5		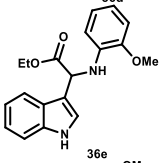 36e	–	–	CH_2Cl_2	rt, 15	75	63
6	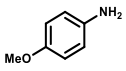	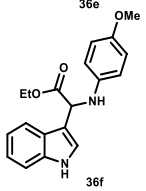 36f	–	$CH_3(CH_2)_{11}OSO_3Na$	H_2O	50, 0.5	98	65
7			–	$Sc(OTf)_3$	CH_2Cl_2	−50, 0.5	88	63
8			$MgSO_4$	–	Toluene	rt, 12	89	68
9			$NaHCO_3$	chiral phosphoric acid	Toluene, H_2O	rt, 0.2; −40, 1.5;	99	64

Table 2. (Continued).

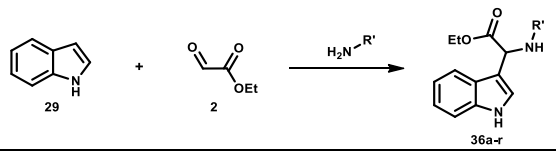

Entry	Reactant (amine)	Product	Reaction conditions				Yields [%]	Lit.
			Reagents	Catalyst	Solvent	T [°C], t [h]		
10	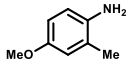	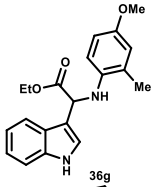 36g	$NaHCO_3$	chiral phosphoric acid	toluene, H_2O	rt, 0.2; −50, 1.5;	92	64
11		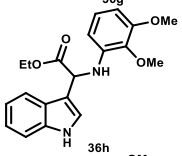 36h	–	$Sc(OTf)_3$	CH_2Cl_2	−50, 12	73	70
12	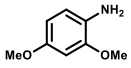	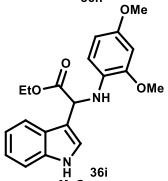 36i	–	$Sc(OTf)_3$	CH_2Cl_2	−50, 0.5	98	63
13	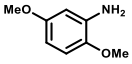	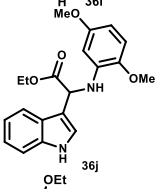 36j	–	–	CH_2Cl_2	rt, 6	54	63
14			–	$Sc(OTf)_3$	CH_2Cl_2	−50, 6	35	63
15	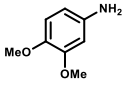	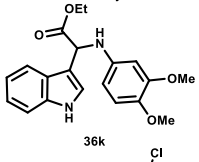 36k	–	–	CH_2Cl_2	rt, 24	55	70
16	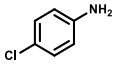	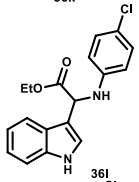 36l	–	$CH_3(CH_2)_{11}OSO_3Na$	H_2O	50, 0.4	96	65
17			–	–	CH_2Cl_2	rt, 24	75	63
18	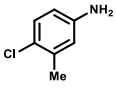	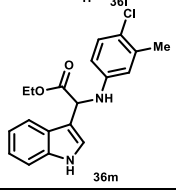 36m	–	$Sc(OTf)_3$	CH_2Cl_2	−50, 12	83	70

Table 2. (Continued).

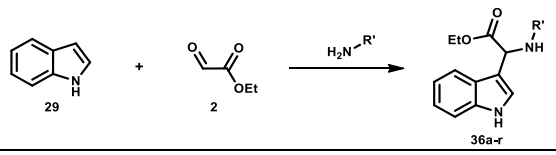

Entry	Reactant (amine)	Product	Reaction conditions				Yields [%]	Lit.
			Reagents	Catalyst	Solvent	T [°C], t [h]		
19	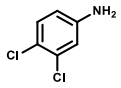	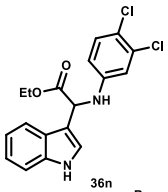 36n	–	$Sc(OTf)_3$	CH_2Cl_2	−50, 12	93	70
20	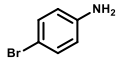	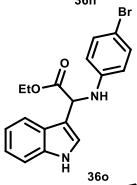 36o	–	$CH_3(CH_2)_{11}OSO_3Na$	H_2O	50, 0.4	88	65
21	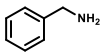	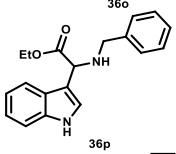 36p	–	$CH_3(CH_2)_{11}OSO_3Na$	H_2O	50, 0.7	77	65
22			–	–	–	rt, 0.5	80	69
23			$MgSO_4$	–	Toluene	rt, 48	61	68
24			Na_2SO_4	$Yb(OTf)_3$	CH_2Cl_2	–, –	82	66
25	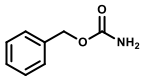	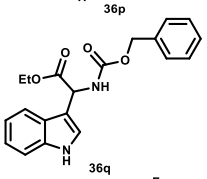 36q	CH_3COCl, $NaHCO_3$	CH_3COOH	$CHCl_3$, H_2O	60, 12; 0, 2	64	67
26		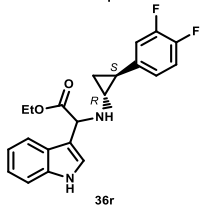 36r	–	–	Toluene, 1,1,1,3,3,3-hexafluoro-2-propanol	rt, 6.5	68	71

enantioselective Friedel–Crafts reaction of indole (**29**) with ethyl glyoxylate imines, therethrough optically active (3-indolyl) glycine derivatives with excellent yields and high enantioselectivities were synthesized (Table 2, entries 9-10).[64] Furthermore, a novel class of potential herbicides, 3-indolylglycines were synthesized via *aza*-Friedel–Crafts in a water/sodium dodecyl sulfate system (Table 2, entries 6, 16, 20-21).[65] To produce unnatural tryptophan derivatives, benzylamine was combined with ethyl glyoxylate to form the intermediate imine which in the presence of catalytic amount of $Yb(OTf)_3$ underwent electrophilic substitution on the 3-position of a variety of indoles (Table 2, entry 24).[66] A novel acetyl chloride-mediated cascade transformation was investigated by a patent using benzyl carbamate, ethyl glyoxylate, and arene nucleophiles (Table 2, entry 25).[67] In addition to the presented experiments,[63–67] the reaction conditions for the further synthesis[68–71] of new 3-indolylglycine derivatives are summarized in Table 2.

Based on the synthetic methods summarized in **Scheme 14**,**15**, when the reactions are catalyzed by 5 mol-% scandium triflate $ScO(Tf)_3$, in cases when, e.g., aniline, 2-methoxyaniline, 2,5-dimethoxyaniline were applied, rearrangements involving the arylamino fragments were observed. In certain cases, these unusual conversions through intermediate **38**, **44** were occurred. The proposed mechanism for the Sc^{III}-catalyzed rearrangements from ethyl 2-(arylamino)-2-(1*H*-indol-3-yl)acetates to the products of the rearrangement

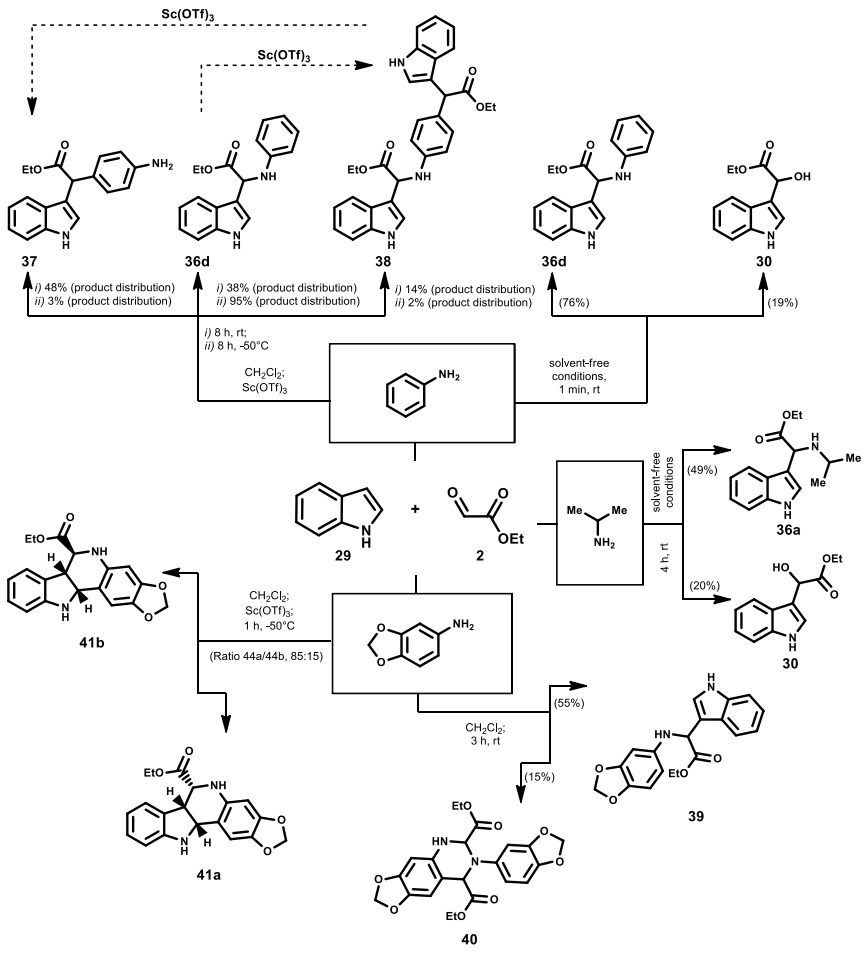

Scheme 14. Synthetic protocols for transformation of indole (**29**) with ethyl glyoxylate (**2**) by applying aniline, propan-2-amine, benzo[*d*][1,3]dioxol-5-amine as amine components.

was reported.[63] Next, the effect induced by the position of a methoxy group on the regioselectivity of the scandium-catalyzed rearrangement of acetates obtained from the multicomponent reaction between indole (**29**), ethyl glyoxylate (**2**), and anilines (e.g., benzo[*d*][1,3]dioxol-5-amine, 3,4-dimethoxyaniline, 3,5-dimethoxyaniline) was defined. It was found that the reaction followed a different pathway, and two pairs of diastereomeric *aza*-Diels–Alder adducts (**42b**, **41a**, **46a** and **42a**, **41b**, **46b**) were isolated.[70] The solvent-free and catalyst-free three-component Friedel–Crafts alkylation of indole (**29**), amines, and ethyl glyoxylate (**2**) was developed for the synthesis of (3-indolyl)glycine derivatives. When aniline and propan-2-amine were used as amine components, the reaction were complete within one minute and 4 h to give the aminoalkylation products **36d, 36a** as well as ethyl 2-hydroxy-2-(1*H*-indol-3-yl)acetate (**30**). It was found that the yield of the reaction was dependent on the addition order of the starting materials. These results prove that the reaction of ethyl glyoxilate with amines is faster than that with indole and that the product of the Friedel–Crafts reaction of indole with in situ generated glyoxylate imine predominates in the solvent-free three-component reaction.[69]

1.3.2. Synthetic Methods Starting from Indole and Glyoxylic Acid

A recent study on the application of indole (**29**) revealed that its reactivity with glyoxylic acid (**11**) has been tested in a few model reactions resulting in 3-formylindole (**32**) (**Scheme 16**). For instance, a highly efficient methodology by electro-chemical decarboxylation of glyoxylic acid using amine (aniline) as a dual function catalyst was reported (method *i*).[72] In addition, photo-redox[73]- (method *ii*) as well as $(NH_4)_2S_2O_8$-mediated[74] (method *iii*) and photochemical[75] (method *iv*) formylation of indole (**29**) using reaction conditions summarized in **Table 3** has been published. The synthesis of C-1 deuterated 3-formylindole **48** by organophotoredox catalyzed direct

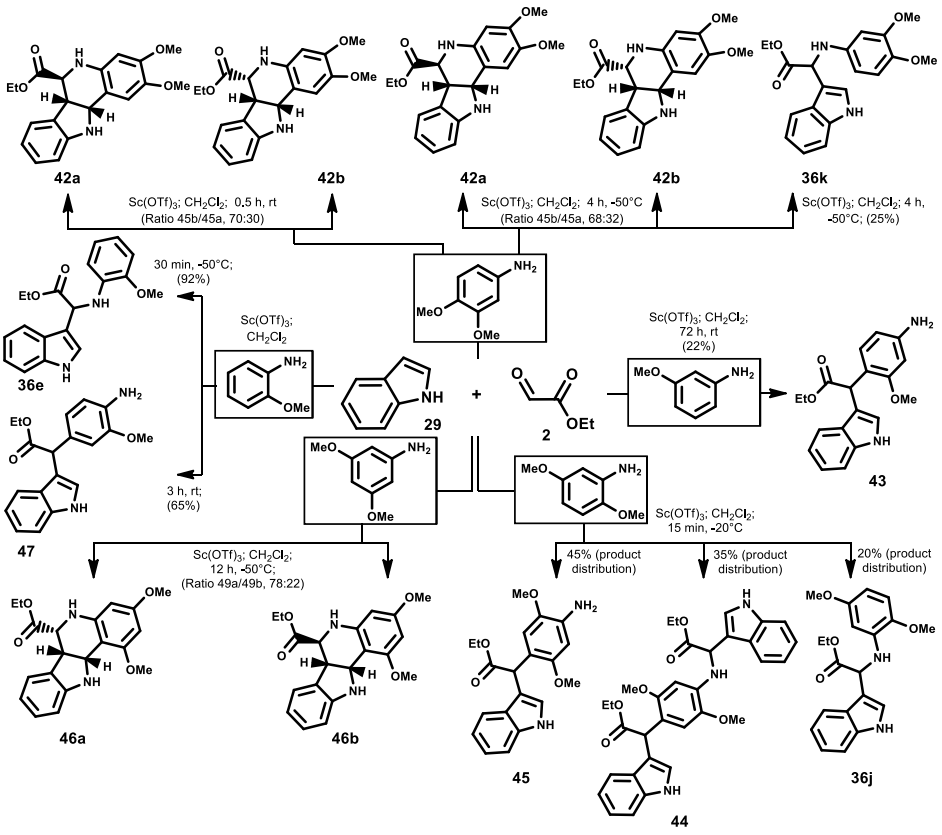

Scheme 15. Reactions between indole (**29**) and ethyl glyoxylate (**2**) by using different anilines with methoxy group(s).

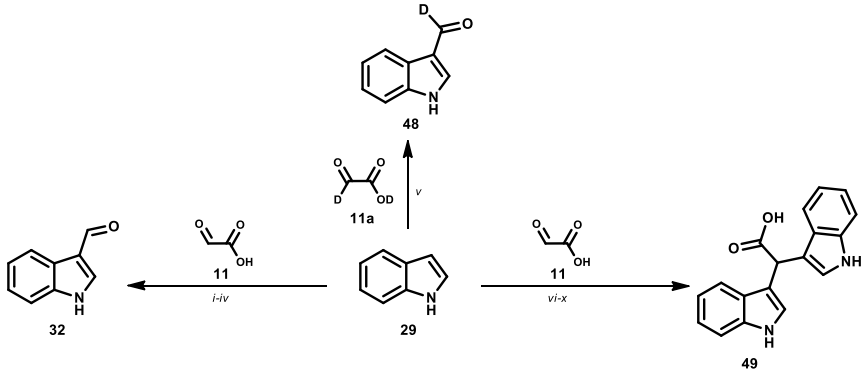

Scheme 16. Preparation of compounds **32**, **48** and **49** by using glyoxylic acid (**11**) or deuterated glyoxylic acid (**11a**).

formylation of indole (**29**) with deuterated glyoxylic acid **11a** was achieved (method *v*).[73] For the synthesis of bis(indolyl)methane derivative **49**, reactions of indole (**29**) with glyoxylic acid (**11**) were carried out in the presence of 1-phenyl-3-(2-pyridyl)thiourea[49] (method *vi*) or zirconium oxychloride octahydrate[76] (method *vii*) or tungstophosphoric acid[77] (method *viii*) or scandium triflate[78] (method *ix*) as catalysts. In addition a patent revealed the synthesis of bis-heterocyclic compounds and their use as anti-inflammatory agents. Accordingly, one equivalent of indole (**29**) was suspended in water and one equivalent of glyoxylic acid (**11**) was added (method *x*). The mixture was stirred at 85 °C for three hours.[79] Reaction conditions are summarized in Table 3.

Regarding further investigations on transformations of indole skeleton (**Scheme 17**), an efficient methodology for C(sp^2)–*H* sulfonylmethylation of indole using glyoxylic acid (**11**) as the C1 source and sodium sulfinates as the sulfone source was developed.

Table 3. Reaction conditions for the synthesis of derivatives **32**, **48**, and **49**.

Reaction	Reagent	Catalyst	Solvent	T [°C]	t [h]	Yield [%]	Lit.
i	$NaClO_4$	Aniline, platinum foils	$(CH_3)_2SO$, H_2O	rt	7	73	72
ii	CH_3COONa, O_2	–	CH_3CN	rt	84	84	73
iii	$(NH_4)_2S_2O_8$	–	$(CH_3)_2SO$, H_2O	rt	3	72	74
iv	–	–	CH_3CN, H_2O	rt	6	65	75
v	CH_3COONa, O_2	–	CH_3CN	rt	24	67	73
vi	–	1-phenyl-3-(2-pyridyl)thiourea ($C_{12}H_{11}N_3S$)	$C_2H_4Cl_2$	60	–	50	49
vii	–	$ZrOCl_2 \cdot 8H_2O$	EtOH, H_2O	rt	5	90	76
viii	–	tungstophosphoric acid ($H_3[PW_{12}O_{40}]$)	H_2O	rt	4	86	77
ix	–	$Sc(OTf)_3$	CH_3CN	rt	12	88	78
x	–	–	H_2O	85	3	85	79

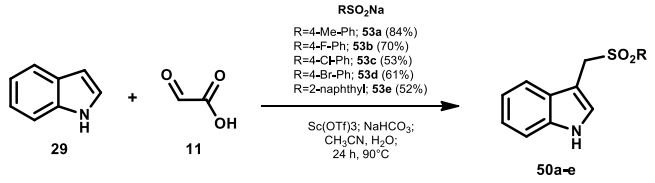

Scheme 17. Method for C(sp^2)–*H* sulfonylmethylation of indole in the presence of $Sc(OTf)_3$.

The reactions were performed in the presence of $Sc(OTf)_3$ (10 mol%) and acetonitrile was applied as solvent.[80]

As depicted by **Scheme 18**, by the reaction of indole (**29**) with glyoxylic acid (**11**) using (+)-tartaric acid-*N,N′*-dimethylurea as a deep eutectic solution, a cascade approach for the synthesis of compound **51** was developed.[81] The synthesis of novel *N*-substituted 3-indolylglycines via three-component Mannich reaction of indole (**29**) and free glyoxylic acid (**11**) in the presence of primary and secondary aliphatic amines was achieved. A series of racemic 3-indolylglycines **52**, **53a**, **53e-f**, **53g-i** using, e.g., methanamine, 2-aminoethanol, prop-2-en-1-amine, benzylamine, *N*-methyl-1-phenylmethanamine, and 2-phenylethanamine as amine components, as well as the optically pure (*S*)-3-indolylglycine using *R*-1-phenylethylamine as chiral pool were synthetized. In the case of latter transformation, precise tuning of reaction conditions using methanol allowed the research group to isolate the major (*R*,*S*)-diastereomer in excellent diastereomeric purity. Regarding the reaction conditions, the

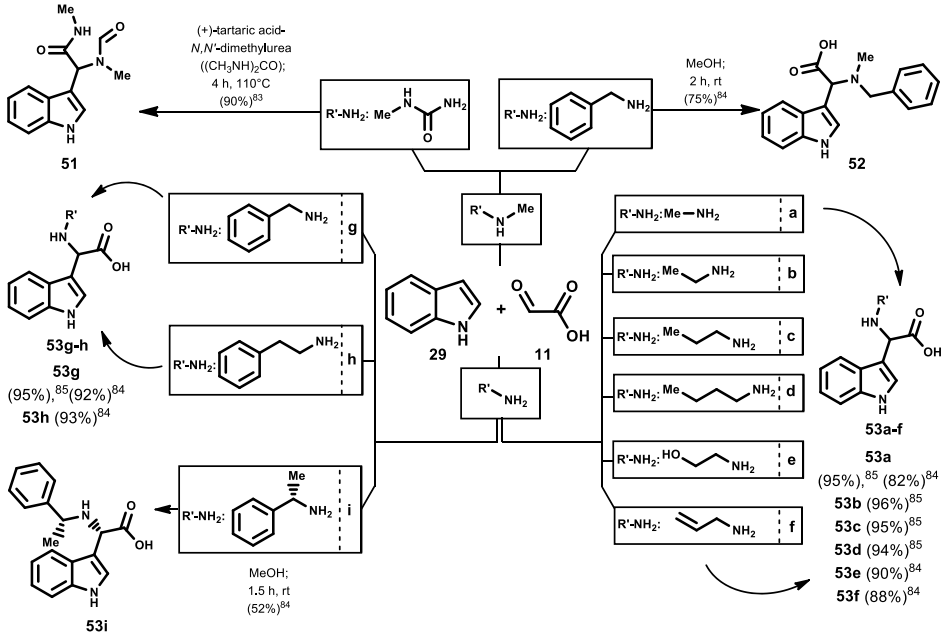

Scheme 18. Synthesis of 5-(indol-3-yl)hydantoin (**51**) and *N*-substituted 3-indolylglycines (**52**, **53a-i**).

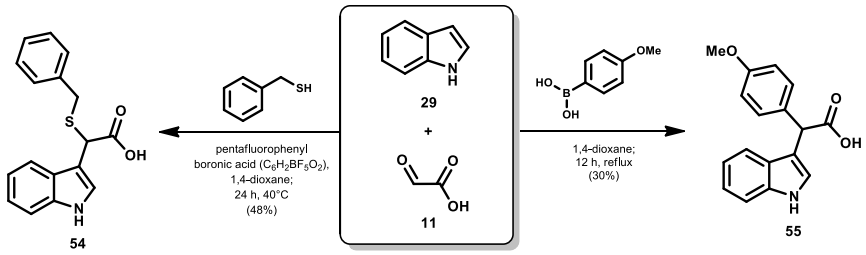

Scheme 19. Applying pentafluorophenyl boronic acid, thiol and (4-methoxyphenyl)boronic acid in the reaction of indole (**29**) and glyoxylic acid (**11**).

transformations were performed in methanol at room temperature.[82] The three-component reaction of primary aliphatic amines, glyoxalic acid (**11**), and indole (**29**) in water at ambient temperature afforded indol-3-yl-glycines **53a-c, 53g**. The procedure is based on the uncatalyzed Friedel–Crafts condensation between indole (**29**) and various iminoacids formed in situ from glyoxalic acid (**11**) and primary aliphatic amines. Among the amines used are methanamine, ethanamine, propan-1-amine, butan-1-amine, and benzylamine.[83]

As further transformation (**Scheme 19**), a novel boronic acid accelerated three-component reaction of indole (**29**), thiol, and glyoxylic acid (**11**) was published, providing a unique class of *α*-sulfanyl-substituted indole derivative **54** containing free carboxylic acids via the formation of *α*-hydroxycarboxylic acids. Additionally, the research group demonstrated that simultaneous activation of the α-hydroxy group with a boronic acid catalyst and internal carboxylic acid is key to promoting the reaction.[84] Furthermore, indoles can serve as substrates for the Petasis boronic acid-Mannich reaction, providing a practical synthetic route for C—C bond formation in α-(*N*-substituted indole)carboxylic acids. When (4-methoxyphenyl)boronic acid was subjected to give the corresponding product **55**, it was obtained in poor yields (30%) after purification.[85]

2. Synthesis of Bioactive Scaffolds via Modified Mannich Reaction

2.1. Preparation of Mannich Bases Substituted with Naphthol and Quinoline Skeleton

2-Naphthol-substituted bifunctional glycine-type precursor was prepared starting from the electron-rich aromatic compound (**1**) and morpholine in the presence of ethyl glyoxylate (**2**) as an aldehyde component (**Scheme 20**).[86] The crude reaction mixtures formed under MW irradiation in 30 min at 80 °C and in 30 min at 100 °C in toluene. By using conventional heating, the formation of the desired product **56** could not be detected. After optimization of reaction conditions, the reaction was repeated, and the presence of two main products was detected; therefore, column chromatographic purification was required. After separation of the desired glycine precursor **56** from side-product **57**, we aimed to investigate the reaction mechanism. The analysis of product **57** indicated the formation of a lactone via intramolecular loss of ethanol. The structure of **57** was verified by comparing the measured characteristic data with the published data.[87] Matuszczak reported the reaction of 2-naphthol and *N*-acetyl-α-hydroxyglycinate furnishing the analog of lactone **57** by using acetic anhydride.[88] In contrast, in our case, the formation of lactone was achieved in situ in toluene under MW irradiation.

As next step, the synthesis of precursor **58** was achieved by reacting 1-naphthol (**18**) as an electron-rich aromatic compound and morpholine with ethyl glyoxylate (**2**) as the aldehyde component (**Scheme 21**).[86] After 1 h in toluene at 80 °C and 40 min at 100 °C under MW irradiation, desired product **58** was formed. The presence of initial compounds was detected; therefore, column chromatographic purification was applied.

Li et al. have developed the first HFIP-promoted denovo synthesis of various nonnatural α-arylated amino esters from readily available amines (such as morpholine), ethyl glyoxylate, and electron-rich arenes (such as 1-naphthol) under mild conditions. Additionally, the possible reaction mechanism was proposed, revealing that the products probably formed via the unstable imine salt intermediates, rather than via the mandelic acid ester intermediates.[62]

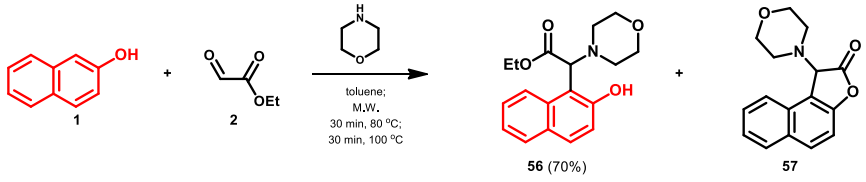

Scheme 20. Synthesis of 2-naphthol-substituted glycine precursor **56**.

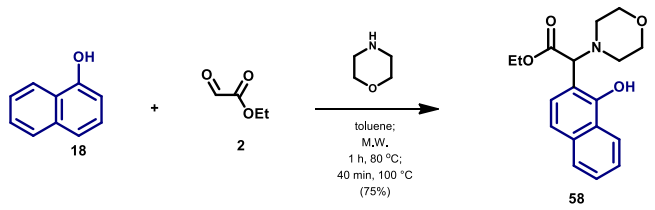

Scheme 21. Preparation of 1-naphthol-substituted glycine precursor **58**.

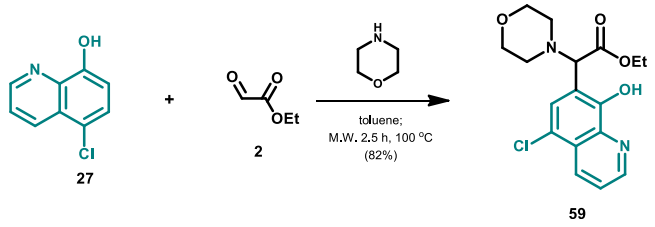

Scheme 22. Application of 5-Cl-8-HQ as electron-rich compound to the synthesis of Mannich base **59**.

8-OHQ is a biologically active moiety[7] interpreted as a potential 1-naphthol analogue. To examine the behavior of 5-Cl-8-HQ in Mannich reaction, derivative **27** was reacted with morpholine in the presence of ethyl glyoxylate (**2**) as an aldehyde component (**Scheme 22**).[89] The formation of a single product and the presence of initial compounds were observed. New compound **59** was isolated and purified by crystallization and recrystallization from iPr$_2$O.

2.2. Transformations of the Synthesized Precursors Substituted with 2-, and 1-naphthol via [4 + 2] Cycloaddition Reactions

In the frame of this study, with aminonaphthol derivative **56** in hand, its reaction with different cyclic imines via [4 + 2] cycloaddition was tested (**Scheme 23**).[86] Mechanistically, during the reaction via loss of morpholine, the presence of partially aromatic *ortho*-quinone methide intermediate has been proved, and it was transformed with different dienophiles to new α-amino acid esters. First, we wanted to investigate the reaction of bifunctional precursor **56** with 3,4-dihydroisoquinoline (**60**)[24] in [4 + 2] cycloaddition. The reaction was performed first at 80 °C under MW irradiation for 60 min in 1,4-dioxane. The progress of the synthesis was monitored that showed the formation of a new spot next to those of the starting materials. By using higher temperatures and longer reactions (100 °C, 300 min), the desired product was isolated in a relatively higher amount. The formation of a single product has been assumed. The relatively weak cross peak on the NOE spectrum of **63** proved that the arrangement of H-7a and H-15 is *trans*. Then we focused on testing the possibility to extend the reaction by using 6,7-dihydrothieno [3,2-*c*]pyridine (**61**)[90] and 3,4-dihydro-*β*-carboline (**62**)[91] as initial cyclic imine dienophiles. The [4 + 2] cycloaddition reactions were performed at 80 and 100 °C in 1,4-dioxane.

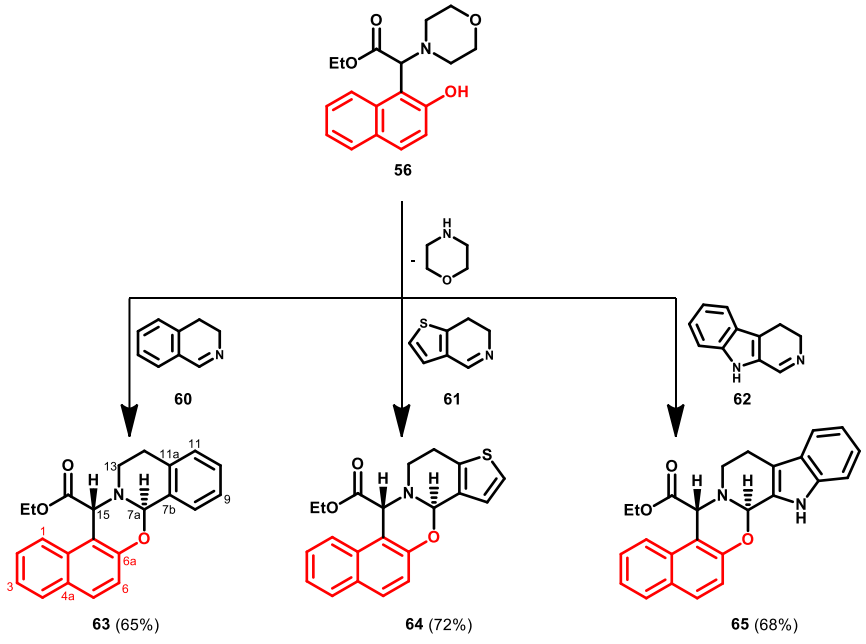

Scheme 23. [4 + 2] Cycloaddition reactions starting from derivative **56**.

Table 4. Reaction conditions for preparation of naphthoxazino derivates via [4 + 2] cycloaddition (**63–65**, **66–68**).

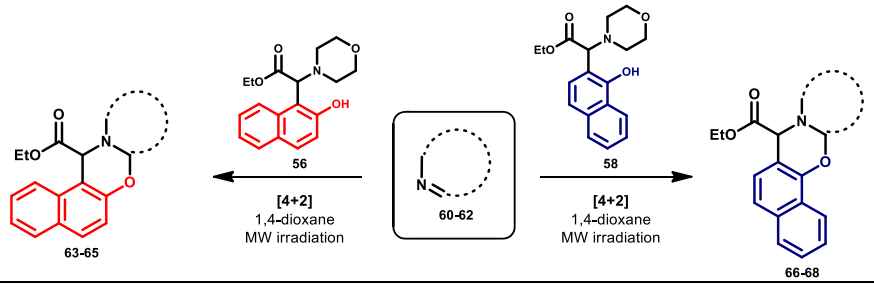

Product	Cyclic imine	Time [min]	Temperature [°C]	Conversion[a] [%]	Yield[b] [%]
63	**60**	60	80	65	
		300	**100**	**73**	**65**
64	**61**	60	80	70	
		280	**100**	**77**	**72**
65	**62**	80	80	67	
		360	**100**	**75**	**68**
66	**60**	20	80	55	
		80	**80**	**70**	**63**
67	**61**	60	100	68	
		80	**100**	**78**	**70**
68	**62**	20	80	65	
		40	100	72	
		260	**120**	**75**	**68**

[a]Determined from crude NMR spectra; [b]Isolated yields. Work-up was performed in the case of each product from its reaction at the highest conversion.

All reactions led to the formation of a single product. In order to separate the desired polycycles from unreacted starting materials, column chromatographic purification was required. Finally, the target compounds were isolated by crystallization. In the case of [4 + 2] cycloaddition, 100 °C and reaction times of 280–360 min were found to be the optimal reaction conditions (**Table 4**). The relative configurations of the newly formed stereogenic center s were proved to be *trans*. Comparing the reactivity of cyclic imines (3,4-dihydroisoquinoline (**60**), 6,7-dihydrothieno[3,2-c] pyridine (**61**), and 3,4-dihydro-*β*-carboline (**62**), the reaction of **61** gave compound **64** isolated as a pure product in a relatively good yield of 72%.

Analogously, by extending the modified Mannich reaction, the stabilization of aminonaphthol derivative **58** via partially aromatic *ortho*-quinone methide intermediate was tested with different cyclic imines in [4 + 2] cycloaddition (**Scheme 24**).[86] Accordingly, 1-naphthol-substituted glycine precursor **58** was reacted with 3,4-dihydroisoquinoline (**60**) at 100 °C under MW irradiation in 1,4-dioxane. After a reaction time of 80 min, the formation of two new spots in TLC were observed. The decomposition of the desired naphthoxazino derivative **66** was observed. The separation of product **66** from the side product was achieved by using column chromatographic purification. Next, we focused on avoiding the formation of the side product by controlling reaction conditions. Therefore, the reaction was repeated at lower temperature (80 °C). The progress of synthesis was monitored in every 20 min showing the formation of a single product after 80 min. After optimizing reaction conditions, the crude reaction mixture was purified by column chromatography.

Taking into consideration of previous experiments, we wanted to investigate the behavior of other dienophiles in [4 + 2] cycloaddition, namely 6,7-dihydrothieno[3,2-*c*]pyridine (**61**) and 3,4-dihydro-*β*-carboline (**62**) (Table 4). The formation of a single product was observed. In the case of newly formed stereogenic centers via [4 + 2] cycloaddition, NOE measurements proved that the relative configuration is *trans*. In conclusion, 80–120 °C and reaction times of 80–260 min were found to be the optimal reaction conditions. Purification of crude mixtures was achieved by column chromatography.

As observed on the performed investigations, although longer reaction times and a higher temperature accelerated the [4 + 2] cycloaddition reactions, conversions were maximized at around 78%. Based on our results, the transformation of new α-amino acid esters seemed to proceed under equilibrium conditions. Accordingly, morpholine, because of its nucleophilic property, is able to stabilize *ortho*-quinone methide to recover the initial aminonaphthol derivative thereby inhibiting [4 + 2] cycloaddition.

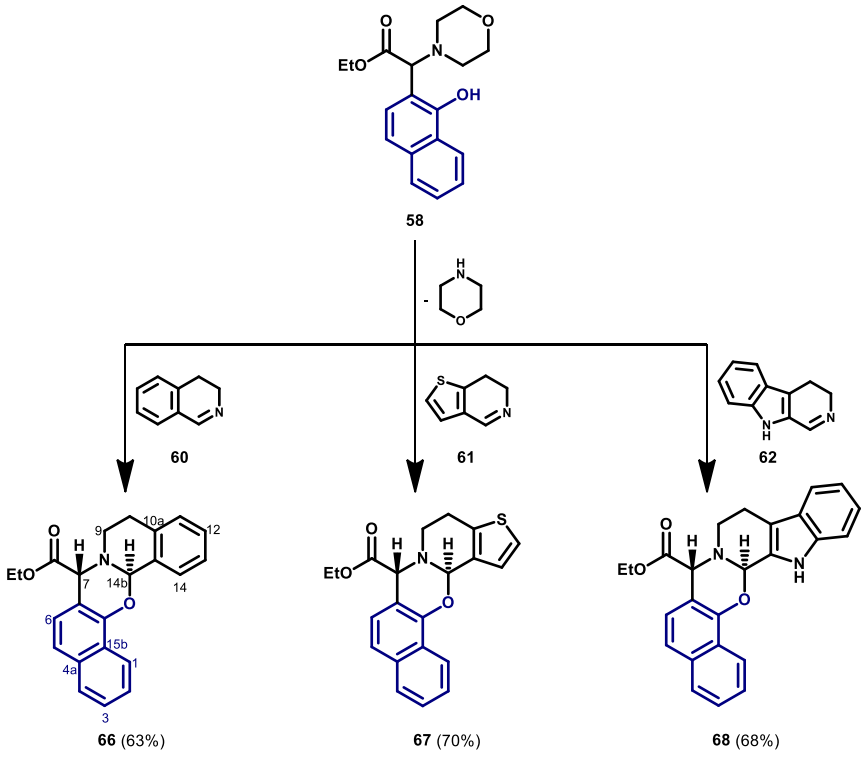

Scheme 24. [4 + 2] Cycloaddition reactions starting from derivative **58**.

2.3. Synthesis of Indole and Naphthol or 8-Hydroxyquinolin Skeleton Containing Di- or Triarylmethane Derivatives

2.3.1. Arylation of Ethyl 2-(2-hydroxynaphthalen-1-yl)-2-morpholinoacetate and Ethyl 2-(1-hydroxynaphthalen-2-yl)-2-morpholinoacetate with Indole or 7-Azaindole

The indole skeleton proves to be a potent biological moiety,[92] and the structure–activity relationships trough structural modifications were examined.[20–23] Taking into consideration of recent investigations that glycine derivatives substituted with 2- and 1-naphthol were found to be excellent precursors to participate in [4 + 2] cycloaddition with different cyclic imines, we desired to test their reactivity with indole and 7-azaindole (**Scheme 25**).[89] Having in hand 2-naphthol-substituted glycine precursor **56** reported previously and indole (**29**), the reaction was performed at 100 °C in 1,4-dioxane under MW conditions. *p*-Toluenesulfonic acid (*p*-TSA) is considered to be an acid catalyst applied frequently in the modified Mannich reaction,[39] we decided to investigate its effect on the reaction. After a reaction time of 1.5 h, the formation of **70** through ester intermediate was observed. The synthesis of 1-(1*H*-indol-3-yl)naphtho [2,1-*b*]furan-2(1*H*)-one (**70**) was already described by Jadhav et al. utilizing a different synthetic pathway, starting from ethyl2-(4-fluorophenylamino)-2-(1*H*-indol-3-yl) acetate and 2-naphthol using scandium triflate in 1,2 dichloroethane via arylation–cyclization.[93] Applying different reaction conditions (modification of solvent, temperature, and additive) led to the same product. In our next experiment, precursor **56** was reacted with 7-azaindole (**69**) in the presence of 10 mol% *p*-TSA at

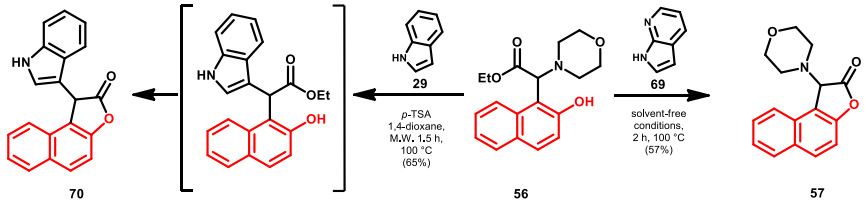

Scheme 25. Reactions of 2-(2-hydroxynaphthalen-1-yl)-2-morpholinoacetate (**56**) with indole (**29**) and 7-azaindole (**69**).

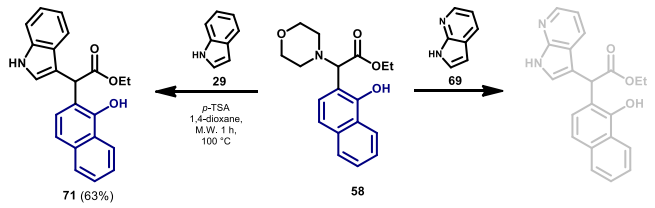

Scheme 26. Preparation of target compound **71** from 1-naphthol-substituted precursor **58**.

100 °C under MW irradiation in 1,4-dioxane, we concluded that the synthesis did not result in the desired derivative. When the reaction was repeated in toluene as solvent, the formation of a multi-spot reaction mixture was monitored. Unfortunately, the desired product could not be isolated even by using column chromatography. Next, the reaction was carried out in solvent-free conditions under MW irradiation at 100 °C. The formation of a lactone structure (compound **57**) via intramolecular loss of ethanol was assumed. The formation and structure of this lactone as side-product was reported in our previous examinations (Chapter 2.1.).

According to the findings on the field of transformation of 2-naphthol-substituted precursor **56** with indole and 7-azaindole, the protocol was further extended for testing the reaction from 1-naphthol-substituted precursor **58** (**Scheme 26**).[89] Accordingly, **58** and indole (**29**) were reacted in the presence of 10 mol% *p*-TSA at 100 C for 60 min under MW irradiation in 1,4-dioxane. The progress of the synthesis was monitored by TLC showing the formation of a new spot. The formation of **71** as a single product was assumed. On the basis of previous observations, the reaction was carried out under other conditions as well, applying toluene as solvent in the presence of 10 mol% *p*-TSA. However, formation of the desired product did not take place. A similar result was found by running the reaction under solvent-free conditions. In favor of examining the possibility of extending the reaction scope, 7-azaindole (**69**) was reacted with precursor **58**. However, even by applying different solvents (toluene, 1,4-dioxane), using solvent-free conditions, and testing different temperatures (80, 100, 120, 150), the target compound did not form.

2.3.2. Arylation of 8-Hydroxyquinoline Skeleton Containing Precursors with Indole or 7-Azaindole

In order to investigate the scope and limitations of the reaction, the synthesis of new diarylmethane derivatives starting from a precursor substituted with 8-OHQ skeleton as well as indole and 7-azaindole was accomplished.[89] The preparation of **72** starting from **59** and indole (**29**) in the presence of 10 mol% *p*-TSA was achieved (**Scheme 27**). In this case, **72** was isolated with a yield of 70% in 4 h at 120 °C. To study the scope and limitations of the reaction, the synthesis of **73** was planned through the reaction of the precursor **59** with 7-azaindole (**69**). The reaction was tested first in toluene at 120 °C by monitoring the conversion of the starting compounds. Since the yield was not satisfactory, the reaction was repeated at 150 °C (Scheme 27). By using higher temperature and longer reaction (3 h), the desired product was isolated by crystallization from the reaction mixture.

To study the effect of the aldehyde component on the synthetic pathway, 5-Cl-8-HQ and morpholine were fixed, and the aldehyde moiety was varied among benzaldehyde and paraformaldehyde.[89] The re-synthesis of precursors **74** was achieved based on the previously published synthetic method.[94] When precursor **74** was reacted with indole (**29**) at 150 °C for 4 h, the desired triarylmethane **75** was isolated in a yield of 67% after purification by column chromatography (**Scheme 28**). In contrast, the reaction between **74** and 7-azaindole (**69**) did not show any transformation upon testing various reaction conditions (solvent, reaction time, and reaction temperature) (Scheme 28).

Next, we focused our efforts to investigate the transformations of precursors that were originally prepared from paraformaldehyde as the aldehyde component.[89] For this reason, the re-synthesis of Mannich base **76** was accomplished applying a synthetic method published previously.[94] Starting from precursor **76** and indole (**29**) and 7-azaindole (**69**), the formation of target compounds **77** and **78** was isolated with low yield in relatively long reactions at high temperatures (**Scheme 29**).

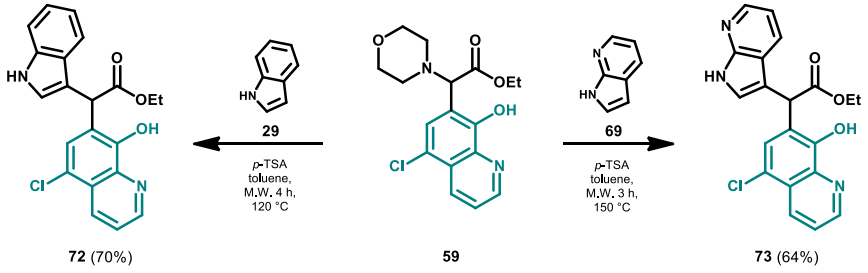

Scheme 27. The transformation of compound **59** bearing the 5-chloro-8-hydroxyquinoline moiety with indole (**29**) and 7-azaindole (**69**).

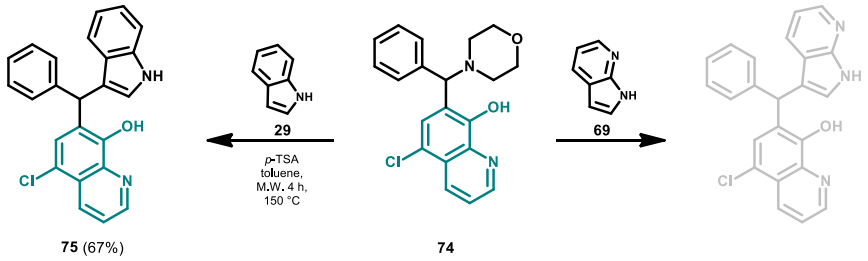

Scheme 28. The reaction of precursor **74** with indole (**29**) and 7-azaindole (**69**).

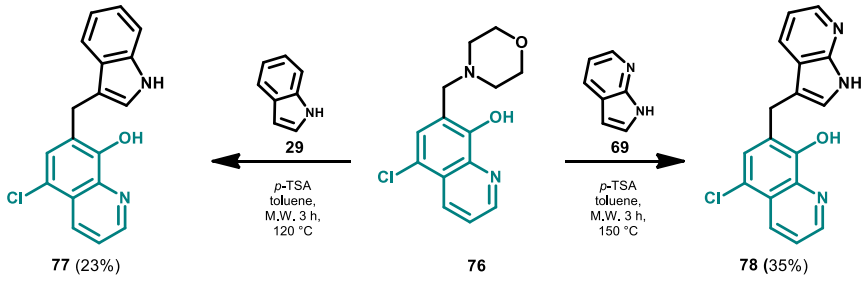

Scheme 29. The transformation of **76** containing paraformaldehyde as aldehyde component.

Since compound **77** is postulated to be formed in the reaction of indole with *ortho*-quinone methide evolving from Mannich base **76**, we carried out a systematic investigation of the synthesis of **77**.[89] According to previous observations, the amine moiety of the Mannich base can be interpreted as a leaving group. Consequently, two precursors have been selected. These were compound **76** bearing the morpholine skeleton and Mannich base **79** having the L-proline motif. This latter precursor was re-synthesized by using our synthetic pathway published earlier,[95] starting from 5-chloro-8-hydroxyquinoline, L-proline, and aqueous formaldehyde. The parallel arylation of precursors **76** and **79** with indole was also investigated (**Scheme 30**).

The reaction offered a possibility to compare the effect of the leaving groups on conversion (**Figure 1**). The reaction was monitored in every 30 min. These systematic investigations allowed us to conclude that starting from precursor **79** the desired diaryl derivative was formed in higher conversion. This may be explained by the better leaving group character of L-proline compared with that of morpholine.[89]

3. Systematically Designed Series of Cyclic Amines Coupled Indole and Azaindole Derivatives

Recent investigations pointed out the scope and limitations of the modified *aza*-Friedel–Crafts reaction by direct coupling of different cyclic imines and indole derivatives as electron-rich aromatic compounds have been examined.[24–26] In addition,

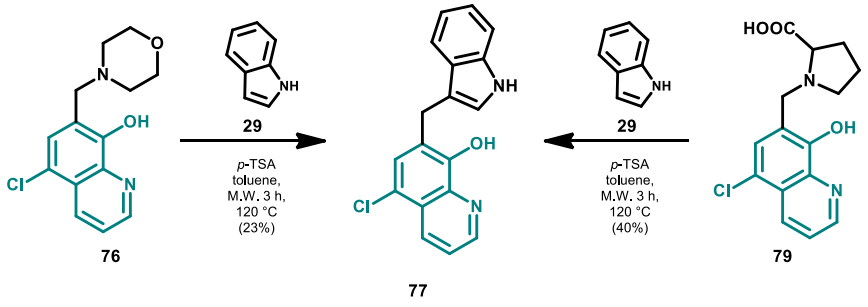

Scheme 30. Synthesis of compound **77** starting from different precursors.

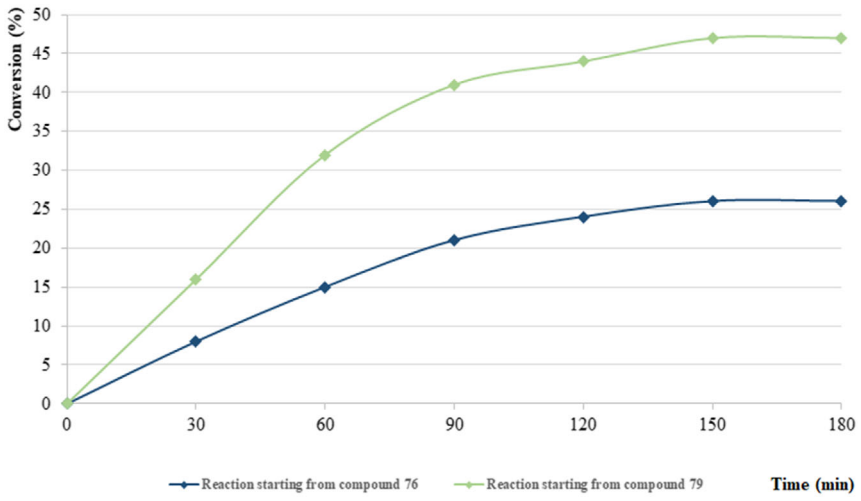

Figure 1. Systematic investigation on compound **76** and **79** to determine the effect of the leaving groups.

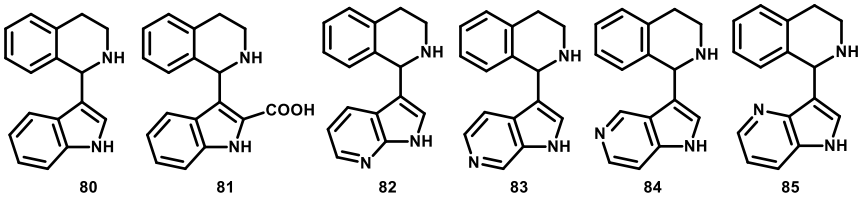

Figure 2. C-1 substituted 1,2,3,4-tetrahydroisoquinolines.

regarding the widespread biological activity of the indole skeleton or their application as pharmaceuticals,[96] we desired to perform a systematic biological examination of 3-isoquinolyl-, 3-thieno[3,2-*c*]pyridyl-, 3-*β*-carbolinyl-, and 3-benz[*c*]azepinyl-indole and -azaindole derivatives. In favor of drawing the inference, we decided to resynthesize the selected derivatives and to extend the synthetic pathway to the preparation of new derivatives to have a preliminary overview about the structure–activity relationship for C-3-coupled indole and azaindole derivatives.[97]

First, in order to examine the effect of the indole skeleton in primary biological screening (**Figure 2**), the isoquinoline part was stabilized and the C-1 coupled (relative to tetrahydroisoquinoline core) indole moiety was varied among indole, indole-2-carboxylic acid, and 4-, 5- and 6-azaindoles (Figure 2). The synthesis of 3-(1,2,3,4-tetrahydroisoquinolin-1- yl)indole (**80**) and 3-(1,2,3,4-tetrahydroisoquinolin-1-yl)indole-2-carboxylic acid (**81**) was accelerated under MW irradiation as described earlier by our research group.[24] To investigate the role of the heteroatom (nitrogen) on the activity, 3-(1,2,3,4-tetrahydroisoquinolin-1-yl) azaindoles (**82-85**) have also been resynthesized.[26]

As further step, we selected compounds **86-90**, with the indole skeleton connected to varied partially saturated cyclic amines, to investigate the influence of the cationic centre (amine) on the biological activity (**Figure 3**).[97] The selected derivatives were synthesized based on the research protocol published previously by direct *aza*-Friedel–Crafts reaction of indole with 6,7-dimethoxy-3,4-dihydroisoquinoline, 6,7-dihydrothieno[3,2-*c*] pyridine, and 4,6-dihydro-3*H*benzo[*c*]azepine and 4,9-dihydro-3*H*-*β*-carboline.[24,25] MW irradiation, as the optimal reaction condition, has been used that led to the formation of the desired **86-89** products in good yields. Recently, the applicability of (4*aR*,8*aR*)-4*a*,5,6,7,8,8*a*-hexahydroquinoxalin-2(1*H*)-one as chiral imine in the modified aza-Friedel–Crafts reaction has been tested by Iwanejko et al.[98] Compounds **90a** and **90b** were synthesized followed by isolation (separation) by column chromatography and determining the absolute configuration of the newly generated asymmetric centre. This allowed to identify the diastereomers by comparing the published characteristic data of **90a** and **90b** with those measured.[98]

Regarding the biological activity of the azaindole skeleton, 7-azaindole derivatives have been found to be a hingebinding element in kinase inhibition.[99] Mechanistically, because of its structural characteristics, 7-azaindole is able to form bidentate hydrogen bonds with the hinge region of kinase. Vemurafenib has been described as 7-azaindole-based kinase drug for the treatment of melanoma.[100] Accordingly, our next

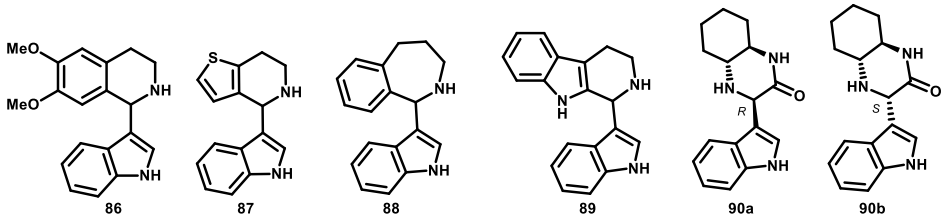

Figure 3. C-3-substituted indole derivatives.

selected set of compounds was designed with the 7-azaindole skeleton connected to partially saturated cyclic amines. The direct coupling of 7-azaindole with cyclic imines, such as 6,7-dihydrothieno[3,2-*c*]pyridine, 3,4-dihydro-*β*-carboline and 4,5-dihydro-3*H*-benz[*c*]azepine, was performed utilizing the solvent-free method previously described leading to the formation of compounds **92-94** (**Figure 4**).[26]

In order to have an overview about the influence of the dimethoxy-substituents tetrahydoisoquinoline skeleton on activity, 3-(6,7-dimethoxy-1,2,3,4-tetrahydroisoquinolin-1-yl)-7-azaindole (**91**) as new precursor was also synthesized starting from 6,7-dimethoxy-3,4-dihydroisoquinoline as cyclic imine and 7-azaindole (**69**). The reaction was performed under solvent-free conditions by applying MW irradiation (2.5 h, 100 °C; 1 h, 110 °C) as the optimal condition (**Scheme 31**).[97]

In the framework of a further structural modification, we wanted to observe the effect of saturated nonracemic cyclic amine coupled with 7-azaindole. Accordingly, 7-azaindole (**69**) and 1.0 equivalent of (4*aR*,8*aR*)-4*a*,5,6,7,8,8*a*-hexahydroquinoxalin-2(1*H*)-one as chiral imine were reacted at room temperature in dichloromethane. After a relatively long reaction (23 h), the appearance of both possible products **95a** and **95b** was detected. In this case, the ratio of **95a**:**95b** was found to be 5:1. Since the conversion was not satisfactory, the synthesis was repeated by using a twostep MW reaction (1.5 h, 40 °C; 1.5 h, 50 °C). A further increase of the temperature (100 °C) under MW conditions resulted in the formation of **95a** and **95b** in a conversion of 57%. Before the work-up procedure, the diastereomeric ratio of **95a**:**95b** was also measured and found to be 5:1 again. It means that the diastereoselectivity of the reaction is not influenced by the reaction temperature (**Table 5**).[97] The desired products **95a** and **95b** were isolated by column chromatography and the configurations of the newly created stereogenic centers (Scheme 31) were determined by comparing the measured characteristic data with the published data found for the analogs **90a** and **90b** (Figure 3).[98]

Regarding the antibacterial activity (**Table 6**), the compounds were tested on Gram-negative *Escherichia coli* and Gram-positive methicillin susceptible and resistant *Staphylococcus aureus* strains. Two derivatives exerted a moderate antibacterial effect on the

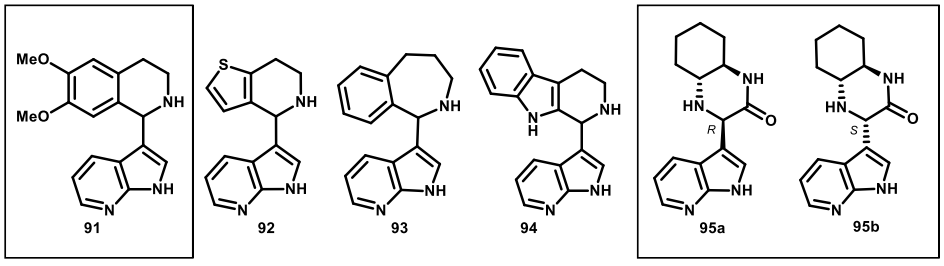

Figure 4. C-3-substituted 7-azaindole derivatives.

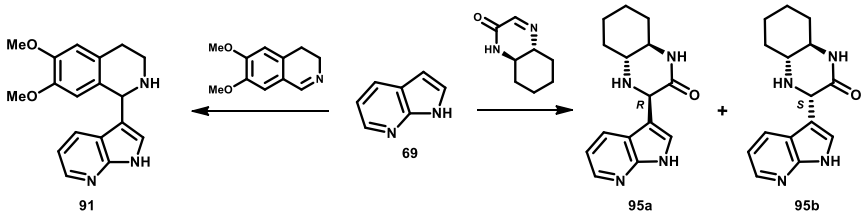

Scheme 31. Synthesis of new derivatives starting from 7-azaindole (**69**) as an electron-rich aromatic compound.

Table 5. Reaction conditions for the synthesis of 3-[(1*R*,4*R*,6*R*)-3-oxo-2,5-diazabicyclo[4.4.0]dec-4-yl]-7-azaindole (**95a**) and 3-[(1*R*,4*S*,6*R*)-3-oxo-2,5-diazabicyclo[4.4.0]dec-4-yl]-7azaindole (**95b**).

Entry	Time [h]	Heating technique	Temperature [°C]	Conversion[a)] [%]	*d.r.*
1	23	Classical heating (oil bath)	Room temperature	11	**95a**:**95b** 5:1
2	1.5	MW	40	9	**95a**:**95b** 5:1
	1.5		50		
3	1.5	MW	80	12	**95a**:**95b** 5:1
4	2	MW	100	57	**95a**:**95b** 5:1

[a)]Determined from crude NMR spectra.

Table 6. Antibacterial effectivity of synthesized compounds.

Entry	Product	Structure	Antibacterial activity									
			Anti-biofilm activity *E. coli* AG100[a)] *S. aureus* MRSA 272123[b)]					RFI				
			cc. [μM, μg/mL]	AV.	SD	comp. OD	Inh. [%]	cc. [μM]	*E. coli* AG100	*E. coli* AG100A	*S. aureus* ATCC 25923	*S. aureus* MRSA 272123
1	**80**	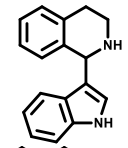	50	0.96[a)]	0.42[a)]	0.81[a)]	−151.92[a)]	50	0.20	0.52	−0.18	−0.03
			100	0.71[b)]	0.06[b)]	0.55[b)]	−42.08[b)]					
				0.67[a)]	0.09[a)]	0.52[a)]	−62.92[a)]					
				0.89[b)]	0.02[b)]	0.74[b)]	−90.25[b)]					
2	**81**	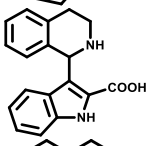	50	0.75[a)]	0.28[a)]	0.60[a)]	−88.57[a)]	50	−0.01	−0.01	−0.14	0.01
			100	0.76[b)]	0.12[b)]	0.61[b)]	−56.75[b)]					
				0.60[a)]	0.10[a)]	0.45[a)]	−40.16[a)]					
				0.78[b)]	0.11[b)]	0.63[b)]	−62.19[b)]					
3	**82**	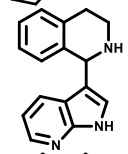	50	0.65[a)]	0.24[a)]	0.50[a)]	−56.12[a)]	50	0.33	0.52	−0.22	0.09
			100	0.68[b)]	0.07[b)]	0.53[b)]	−36.37[b)]					
				0.54[a)]	0.09[a)]	0.39[a)]	−20.45[a)]					
				0.70[b)]	0.25[b)]	0.54[b)]	−39.38[b)]					
4	**83**	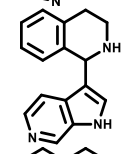	50	0.64[a)]	0.27[a)]	0.49[a)]	−54.32[a)]	50	0.47	0.53	−0.09	0.10
			100	0.64[b)]	0.11[b)]	0.48[b)]	−24.38[b)]					
				0.72[a)]	0.06[a)]	0.57[a)]	−77.10[a)]					
				0.58[b)]	0.08[b)]	0.42[b)]	−8.41[b)]					
5	**84**	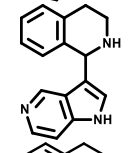	50	0.48[a)]	0.08[a)]	0.33[a)]	−4.03[a)]	50	0.04	0.42	−0.17	0.00
			100	0.71[b)]	0.05[b)]	0.56[b)]	−43.49[b)]					
				0.48[a)]	0.14[a)]	0.32[a)]	−1.37[a)]					
				0.53[b)]	0.07[b)]	0.37[b)]	3.95[b)]					
6	**85**	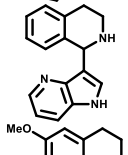	50	0.82[a)]	0.32[a)]	0.67[a)]	−109.61[a)]	50	0.37	0.66	−0.14	0.02
			100	0.65[b)]	0.11[b)]	0.49[b)]	−26.68[b)]					
				0.56[a)]	0.02[a)]	0.40[a)]	−26.63[a)]					
				0.67[b)]	0.13[b)]	0.51[b)]	−31.40[b)]					
7	**86**	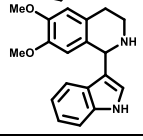	50	0.84[a)]	0.33[a)]	0.69[a)]	−115.71[a)]	50	0.33	0.34	0.17	0.04
			100	0.94[b)]	0.03[b)]	0.78[b)]	−100.97[b)]	100	0.44	0.40	0.38	0.11
				0.51[a)]	0.11[a)]	0.36[a)]	−12.66[a)]					
				0.50[b)]	0.14[b)]	0.35[b)]	10.12[b)]					

Table 6. (Continued).

Entry	Product	Structure	Antibacterial activity								
			Anti-biofilm activity *E. coli* AG100[a] *S. aureus* MRSA 272123[b]					RFI			
			cc. [μM, μg/mL]	AV.	SD	comp. OD	Inh. [%]	cc. [μM]	*E. coli* AG100	*E. coli* AG100A	*S. aureus* ATCC 25923	*S. aureus* MRSA 272123
8	**87**	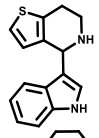	50 100	1.03[a] 0.75[b] 0.63[a] 0.89[b]	0.35[a] 0.12[b] 0.13[a] 0.24[b]	0.88[a] 0.59[b] 0.48[a] 0.74[b]	−174.29[a] −52.76[b] −49.78[a] −89.75[b]	50 100	0.56 0.71	0.43 0.85	0.68 –	0.07 0.17
9	**88**	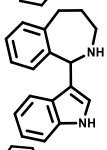	50 100	1.08[a] 0.55[b] 0.67[a] 0.50[b]	0.24[a] 0.03[b] 0.11[a] 0.03[b]	0.93[a] 0.40[b] 0.52[a] 0.35[b]	−189.93[a] −2.23[b] −63.44[a] 9.87[b]	50 100	0.36 0.33	0.36 0.26	0.30 –	−0.09 0.03
10	**89**	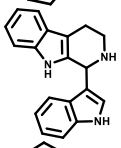	50 100	0.45[a] 0.62[b] 0.48[a] 0.43[b]	0.03[a] 0.08[b] 0.05[a] 0.08[b]	0.29[a] 0.46[b] 0.33[a] 0.28[b]	8.02[a] −18.53[b] −2.78[a] 29.17[b]	25 50 100	– 0.24 0.25	– 0.22 0.36	0.16 – –	– 0.01 −0.10
11	**90a**	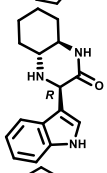	50 100	0.36[a] 0.75[b] 0.47[a] 0.65[b]	0.03[a] 0.06[b] 0.06[a] 0.06[b]	0.21[a] 0.60[b] 0.32[a] 0.50[b]	34.30[a] −53.96[b] 0.04[a] −27.41[b]	50 100	0.20 0.11	0.18 −0.07	0.14 0.24	−0.06 −0.08
12	**90b**	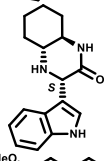	50 100	0.43[a] 0.74[b] 0.37[a] 0.84[b]	0.03[a] 0.05[b] 0.04[a] 0.04[b]	0.28[a] 0.58[b] 0.22[a] 0.68[b]	13.80[a] −49.75[b] 31.45[a] −75.58[b]	50 100	0.17 0.12	−0.10 −0.02	0.05 0.14	−0.02 0.01
13	**91**	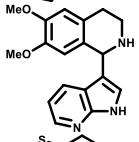	50 100	0.45[a] 0.73[b] 0.35[a] 0.47[b]	0.11[a] 0.07[b] 0.05[a] 0.08[b]	0.30[a] 0.57[b] 0.20[a] 0.31[b]	6.53[a] −47.18[b] 38.34[a] 19.13[b]	50 100	0.27 0.26	0.17 0.40	0.30 0.16	0.02 0.02
14	**92**	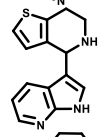	50 100	0.49[a] 0.53[b] 0.43[a] 0.59[b]	0.03[a] 0.01[b] 0.02[a] 0.14[b]	0.34[a] 0.38[b] 0.28[a] 0.44[b]	−6.06[a] 2.49[b] 12.06[a] −12.95[b]	50	0.06	0.29	−0.10	−0.01
15	**93**	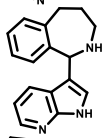	50 100	0.48[a] 0.49[b] 0.45[a] –	0.03[a] 0.07[b] 0.04[a] –	0.33[a] 0.33[b] 0.30[a] –	−3.17[a] 13.90[b] 5.83[a] –	50	0.12	0.57	−0.16	0.06
16	**94**	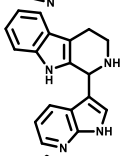	50 100	0.57[a] 0.41[b] 0.41[a] 0.55[b]	0.10[a] 0.28[b] 0.03[a] 0.15[b]	0.42[a] 0.26[b] 0.26[a] 0.39[b]	−32.34[a] 33.38[b] 19.98[a] −1.29[b]	50	0.01	0.30	−0.25	−0.02
17	**95a**	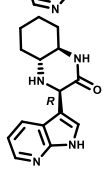	50 100	0.46[a] 0.46[b] 0.41[a] 0.61[b]	0.10[a] 0.01[b] 0.06[a] 0.02[b]	0.31[a] 0.30[b] 0.26[a] 0.46[b]	3.71[a] 21.96[b] 18.73[a] −17.93[b]	50 100	0.17 0.06	0.04 −0.03	−0.01 0.33	0.01 0.02

Table 6. (Continued).

Entry	Product	Structure	Antibacterial activity									
			Anti-biofilm activity *E. coli* AG100[a] *S. aureus* MRSA 272123[b]					RFI				
			cc. [μM, μg/mL]	AV.	SD	comp. OD	Inh. [%]	cc. [μM]	*E. coli* AG100	*E. coli* AG100A	*S. aureus* ATCC 25923	*S. aureus* MRSA 272123
18	**95b**	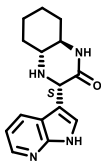	50 100	0.51[a] 0.52[b] 0.42[a] 0.57[b]	0.09[a] 0.26[b] 0.03[a] 0.12[b]	0.36[a] 0.37[b] 0.27[a] 0.41[b]	−11.22[a] 4.71[b] 14.82[a] −5.75[b]	50 100	0.17 −0.01	0.30 0.14	0.10 0.12	−0.02 −0.05
CCCP									0.74	0.74	–	–
Reserpine (RES)											0.32	0.23

[a]Determined anti-biofilm activity on *E. coli* AG100 strain; [b]Determined anti-biofilm activity on *S. aureus* MRSA 272123 strain.

reference *S. aureus* strains: **93** and **89** had an MIC of 50 μM. The other derivatives had an MIC of 100 μM or >100 μM on the tested bacterial strains.[97]

Furthermore, the efflux pump inhibiting (EPI) properties of the compounds were assessed on Gram-negative and Gram-positive bacterial strains, such as AcrAB-TolC pump expressing *E. coli* AG100, its AcrAB-TolC-deleted mutant strain *E. coli* AG100A and methicillin susceptible *S. aureus* ATCC 25923 reference strain, methicillin-resistant *S. aureus* MRSA 272123 clinical strains, respectively. The EPI activity was compared to the positive control and in the case of the *E coli* strains, an RFI value above 0.30 was considered as an effective efflux pump inhibitor (the positive control CCCP had an RFI of 0.74 on the pump expressing and pump deleted strains). Compound **82** was effective on *E. coli* AG100 (RFI: 0.33) and caused higher EB accumulation in the mutant *E. coli* strain (RFI: 0.52). Similar activity was obtained on *E. coli* AG100 in the presence of compounds **83** (RFI: 0.47) and **85** (RFI: 0.37). Furthermore, the compounds were also more active on the mutant strain indicating that AcrAB-TolC is crucial in the defense mechanisms of bacteria against toxic compounds. Compounds **86** and **88** were potent EPIs at 50 μM with RFIs of 0.33 and 0.36 on *E. coli* AG100, respectively. Furthermore, their activity was near the same on the mutant *E. coli* strain because they have more targets in the bacterial cells, e.g., membrane destabilizing activity without affecting efflux pumps. The most potent EPI of the AcrAB-TolC system was **87** with RFI of 0.56 on the *E. coli* AG100 strain at 50 μM, and lower activity was observed on the pump mutant strain (RFI: 0.43). On the Gram-positive strains the positive control was reserpine: it was more active on the methicillin susceptible reference strain (RFI: 0.32) than on the MRSA clinical isolate (RFI: 0.23). None of the compounds had EPI properties on the MRSA strain. On the methicillin susceptible strain the most potent EPIs at 50 μM are the following: **87** (RFI: 0.68), **88** (RFI: 0.30), **91** (RFI: 0.30), and **86** (RFI: 0.17). Considering the antibacterial evaluations, the indole skeleton connected with 6,7-dihydrothieno[3,2-*c*]pyridine as a partially saturated cyclic amine has been found to be the most effective (Table 6, Entry 8).

Using the bacterial strains mentioned earlier, the anti-biofilm activity of the derivatives was determined using crystal violet staining. No biofilm inhibition was observed on the pump-deleted mutant *E. coli* AG100A and on the methicillin susceptible *S. aureus* ATCC 25923 strains. Three derivatives could inhibit the biofilm formation of *E. coli* AG100 with inhibition degree of nearly 30%: **91** (inhibition: 38.34%), **90b** (inhibition: 31.45%) at 100 μM and **90a** (inhibition: 34.30%) at 50 μM. Four derivatives could inhibit the biofilm formation of the MRSA strain: the most potent one was **94** demonstrating an inhibition of 33.38% at 50 μM, then **89** with an inhibition of 29.17% at 100 μM. Furthermore, **95a** (an inhibition of 21.96% at 50 μM) and the weakest activity of 19.13% was detected in the presence of **91** at 100 μM. In point of correlation between structure and biological activity, 7-azaindole as an electron-rich aromatic compound could be identified as a significant moiety (Table 6, Entry 13, 16).

The cytotoxic activity of the derivatives was determined using sensitive (Colo 205) and ABCB1 efflux pump expressing (Colo 320) colon adenocarcinoma cell lines and a normal, noncancerous fibroblast cell line MRC-5.[97] The most potent derivatives were **89**, **80**, **87**, **82**, and **88**. The highest anticancer activity was measured in the presence of **87** and **89** on Colo 205 cells (IC_{50}: 21.81 and 24.71 μM, respectively) and Colo 320 cells (IC_{50}: 12.94 and 13.55 μM, respectively). However, compound **89** showed moderate toxicity on normal cells too (IC_{50}: 22.86 μM), whereas compound **87** had no toxic effect on

Table 7. Cytotoxic applicability of prepared derivatives.

Entry	Product	Structure	Cytotoxic activity										
			Colo 205		Colo 320		MRC-5		Inhibition of *P*-glycoprotein				
			IC_{50} [μM]	SD±	IC_{50} [μM]	SD±	IC_{50} [μM]	SD±	cc. [μM]	FSC	SSC	FL-1	FAR
1	**80**	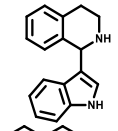	22.37	2.04	30.76	0.86	>100	–	2 20	2010 2032	1041 1026	3.34 6.49	0.86 1.66
2	**81**	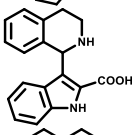	>100	–	53.58	1.52	>100	–	2 20	2016 2016	1041 1024	3.74 2.62	0.96 0.67
3	**82**	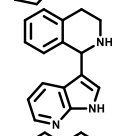	64.35	2.17	53.52	0.90	>100	–	2 20	1621 1594	896 917	9.64 9.75	1.47 1.48
4	**83**	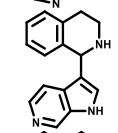	>100	–	>100	–	98.80	2.17	2 20	1999 1963	1045 1027	3.61 3.26	0.92 0.83
5	**84**	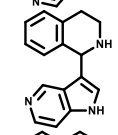	>100	–	>100	–	>100	–	2 20	2033 2054	1042 1038	3.93 2.84	1.01 0.73
6	**85**	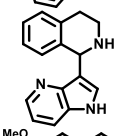	>100	–	>100	–	>100	–	2 20	1633 1623	901 896	6.51 6.58	0.99 1.00
7	**86**	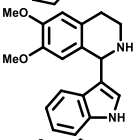	47.38	0.97	60.38	1.61	>100	–	2 20	1612 1591	876 883	15.40 26.60	2.34 4.04
8	**87**	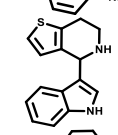	21.81	1.33	12.94	0.26	>100	–	2 20	1615 1618	865 910	6.48 33.80	0.99 5.14
9	**88**	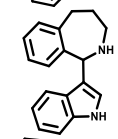	97.85	0.61	41.06	1.20	>100	–	2 20	1609 1596	888 897	7.26 17.10	1.10 2.60
10	**89**	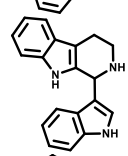	24.71	0.10	13.55	0.98	22.86	0.57	2 20	1643 1627	1030 992	4.13 13.00	0.72 2.26
11	**90a**	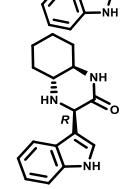	>100	–	>100	–	>100	–	2 20	1655 1629	1028 1041	3.79 3.07	0.66 0.53

Table 7. (Continued).

Entry	Product	Structure	Cytotoxic activity										
			Colo 205		Colo 320		MRC-5		Inhibition of *P*-glycoprotein				
			IC_{50} [μM]	SD±	IC_{50} [μM]	SD±	IC_{50} [μM]	SD±	cc. [μM]	FSC	SSC	FL-1	FAR
12	**90b**	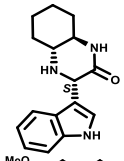	>100	–	>100	–	>100	–	2 20	1670 1636	1014 1043	3.39 3.27	0.59 0.57
13	**91**	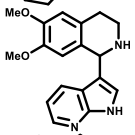	>100	–	>100	–	>100	–	2 20	1669 1668	1040 1036	3.38 2.96	0.59 0.52
14	**92**	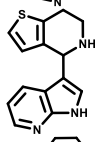	>100	–	>100	–	>100	–	2 20	1974 2007	1009 1058	6.86 7.46	1.76 1.91
15	**93**	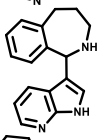	79.56	4.20	68.47	6.06	>100	–	2 20	2014 2006	1024 1017	4.79 12.10	1.23 3.10
16	**94**	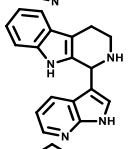	66.79	1.52	54.23	1.70	>100	–	2 20	2025 2023	1011 1022	5.68 6.38	1.45 1.63
17	**95a**	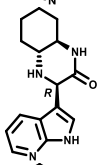	>100	–	>100	–	>100	–	2 20	1652 1639	1016 1040	4.44 3.55	0.77 0.62
18	**95b**	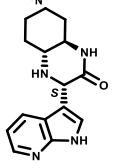	>100	–	>100	–	>100	–	2 20	1660 1662	1033 1048	2.68 2.51	0.47 0.44

normal cells. The IC_{50} values of **80** and **87** were between 10 and 30 μM on the colon adenocarcinoma cells and, fortunately, these derivatives were not toxic on normal MRC-5 fibroblasts ($IC_{50} > 100$ μM). In the case of **82** and **88**, the derivatives were more effective on the resistant cell line (IC_{50} of 53.52 and 41.06 μM, respectively) compared to the sensitive one (IC_{50} of 64.35 and 97.85 μM, respectively). In addition, they were not toxic on normal fibroblasts ($IC_{50} > 100$ μM for both compounds). Derivative **86** was more toxic on the sensitive cells (IC_{50}: 47.38 μM) than on the resistant ones (IC_{50}: 60.38 μM). Compounds **93** and **94** showed mild cytotoxic activity on cancer cells (IC_{50}: 50–80 μM), and they did not affect the viability of normal cells ($IC_{50} > 100$ μM). To conclude, in favor of improved cytotoxic activity, the presence of the indole skeleton and 6,7-dihydrothieno[3,2-*c*]pyridine as well as 3,4-dihydro-*β*-carboline as cyclic imine is relevant (**Table 7**, Entry 8, 10).

Since the difference between the sensitive and resistant colon adenocarcinoma cell lines is the expression of the MDR efflux transporter ABCB1 (*P*-glycoprotein), the activity of the compounds was assessed on the inhibition of ABCB1. The ABCB1 inhibitory activity was compared based on the fluorescence activity ratio (FAR) values at 2 and 20 μM. FAR values above 2 are considered as active ABCB1 modulators. Out of all derivatives, **86**, **87**, **88**, **89**, and **93** showed inhibitory effect. The most potent efflux pump inhibitor (EPI) was **86** showing inhibition in both 2 and 20 μM (FAR: 2.34 and 4.04). The other compounds exerted inhibition only at 20 μM: **87** (FAR: 5.14), **93** (FAR: 3.10), **88** (FAR: 2.60), and **89** (FAR: 2.26).

In the case of inhibition of *P*-glycoprotein, the indole moiety has been described as the most active electron-rich aromatic component. With respect to the coupled cyclic amine side, 6,7-dimethoxyisoquinoline has been interpreted to be a beneficial structural element (Table 7, Entry 7).

4. Biological Evaluations on Synthesized Compounds

The biological evaluations described in this section were carried out by our co-operating and co-author partner Gabriella Spengler. The acquired results show the importance of the synthetic transformations carried out and were deemed worthy of mentioning in a separate paragraph.

4.1. Biological Properties of Synthesized 2- and 1-Naphthol-Substituted Glycine Derivatives and *α*-Amino Acid Esters

In order to examine the biological properties of prepared derivatives, antibacterial and efflux pump inhibiting activities were examined.[86] According to the data no significant antibacterial effect was observed for most of the compounds on either Gram-negative or Gram-positive strains. However, compound **68** exhibited antibacterial effect on the reference *S. aureus* ATCC

Table 8. Efflux pump inhibiting activity of the derivatives on *S. aureus* ATCC 25923 strain.

RFI Concentration	*S.aureus* ATCC 25923		
50 μM	Mean	SD	RFI
56	58168.67	865.83	**1.10**
63	31759.00	1778.37	0.15
64	29306.00	1165.51	0.06
65	27892.33	884.07	0.01
58	11677.33	1308.70	−0.58
66	44414.33	946.94	**0.61**
67	36826.67	2499.36	**0.33**
100 μM	Mean	SD	RFI
56	51721.00	905.77	**0.87**
63	31231.67	894.65	0.13
64	33816.67	3255.64	0.22
65	29131.67	2453.80	0.05
58	7624.33	1372.54	−0.72
66	42864.00	2360.31	**0.55**
67	77859.67	5158.78	1.82
3.125 μM	Mean	SD	RFI
68	34824.33	1646.59	**0.26**
	Mean	SD	RFI
DMSO	27636.67	1089.18	0.00
Reserpine	54056.00	829.47	**0.96**

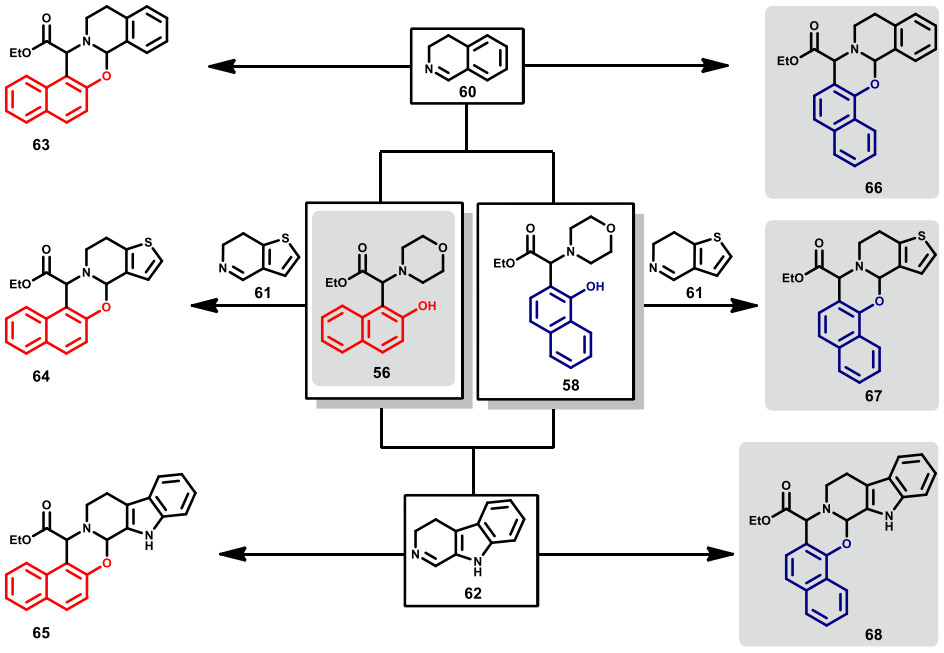

Figure 5. The most effective compounds with antibacterial activity.

25923 strain. The activity of the compounds on efflux pump inhibition can be assessed by real-time fluorimetry applying a fluorochrome (e.g., ethidium bromide), a substrate of the bacterial efflux pumps. Since the compounds, with the exception of **68**, had no antibacterial activity, they were tested at 50 and 100 μM concentrations. In the real-time ethidium bromide accumulation assay, compounds with an efflux pump inhibitory (EPI) effect have a higher relative fluorescence index (RFI) compared to that of the untreated control. The derivatives were not effective on the Gram-negative *Escherichia coli* AG100 strains. However, they had potent EPI activity on the susceptible and resistant *S. aureus* strains (**Figure 5**). In the case of the susceptible reference *S. aureus* ATCC 25923, **56** and **66** were effective EPIs at 100 μM. In addition, **56**, **66**, and **67** showed EPI activity at 50 μM. Since **68** had antibacterial activity on this *S. aureus* strain, the compound was applied at MIC/2 concentration and presented an RFI of 0.26 (**Table 8**).

With respect to the resistant *S. aureus* MRSA ATCC 43300, **66** and **67** were effective at both concentrations tested (**Table 9**).

Table 9. Efflux pump inhibiting activity of the derivatives on *S. aureus* MRSA ATCC 43300 strain.

Concentration	*Staphylococcus aureus* MRSA ATCC 43300		
50 μM	Mean	SD	RFI
56	87762.67	3187.90	0.12
63	92734.00	528.62	0.19
64	88184.67	666.65	0.13
65	76072.00	1171.02	−0.03
58	56126.33	299.38	−0.28
66	111300.67	1782.32	**0.43**
67	101450.33	1316.67	**0.30**
68	84683.00	455.64	0.09
100 μM	Mean	SD	RFI
56	84280.00	1539.30	0.08
63	93822.67	4081.38	0.20
64	88655.67	1118.00	0.14
65	78009.00	1574.59	0.00
58	18886.00	648.23	−0.76
66	114226.00	744.67	**0.46**
67	103410.00	1139.71	**0.33**
68	90479.33	1534.61	0.16
	Mean	SD	RFI
DMSO	78039.33	1254.261	
Reserpine	101532.7	3878.731	**0.30**

4.2. Biological Activity of Indole and 8-Hydroxyquinoline, 2- and 1-naphthol skeleton containing di- or Triarylmethane Derivatives

Regarding the obtained results, the compounds showed a potent toxic activity against the sensitive Colo205 and resistant Colo320 cell lines (IC_{50} values were between 1.72 and 53.64 μM) (**Table 10**).[89] Overall, it was observed that the tested compounds were more effective on the Colo320 cell line, with the exception of the compound **75**. Compounds **71** and **70** showed no effect on Colo205 cells, and **70** had no effect on Colo320 either. Only derivatives **72**, **73**, and **75** exerted a mild cytotoxic effect on the normal MRC-5 cell line compared to the cancer cell lines. This means that the compounds can be

Table 11. Selectivity indexes (SI) and relative resistance (RR) of the compounds.

	MRC-5/Colo205	MRC-5/Colo320	Colo320/Colo205
	SI		RR
70	–	–	NA
71	–	NA	NA
59	>6	>6	0.83
72	11.2	11.4	0.98
73	5.7	9.1	0.62
75	11.7	11	1.07
77	>6	>6	0.37
78	NA	NA	0.57

Table 10. Cytotoxic effect of the compounds on sensitive (Colo205) and resistant (Colo320) colon adenocarcinoma and MRC-5 normal embryonal fibroblast cell lines. Doxorubicin was used as a positive control. AV: average of 3 parallel experiment, SD: standard deviation.

Colo205 [μM]						Colo320 [μM]					MRC-5 [μM]			
				AV.	SD				AV.	SD			AV.	SD
70	–	–	–	**>100**	–	–	–	–	**>100**	–	–	–	**>100**	–
71	–	–	–	**>100**	–	53.82	54.92	52.18	**53.64**	1.38	–	–	**>100**	–
59	2.07	2.06	2.02	**2.05**	0.02	1.565	1.813	1.79	**1.72**	0.14	–	–	**>100**	–
72	5.51	4.71	4.42	**4.88**	0.56	4.636	4.832	4.957	**4.81**	0.16	54.46	55.08	**54.77**	0.44
73	8.05	7.42	8.84	**8.11**	0.71	5.157	4.923	5.109	**5.06**	0.12	46.9	45.56	**46.23**	0.95
75	2.49	2.49	2.63	**2.53**	0.08	2.552	2.84	2.781	**2.72**	0.15	30.08	29.28	**29.68**	0.57
77	13.56	13.37	12.26	**13.06**	0.70	4.967	4.74	4.91	**4.87**	0.12	–	–	**>100**	–
78	36.49	39.42	40.40	**38.77**	2.03	22.98	21.89	22.54	**22.47**	0.55	–	–	**>100**	–
DOX	0.84	0.89	0.81	**0.85**	0.04	3.117	3.12	2.961	**3.07**	0.09	–	–	**>8.62**	–
DMSO	–	–	–	**>2%**	–	–	–	–	**>2%**	–	–	–	**>2%**	–

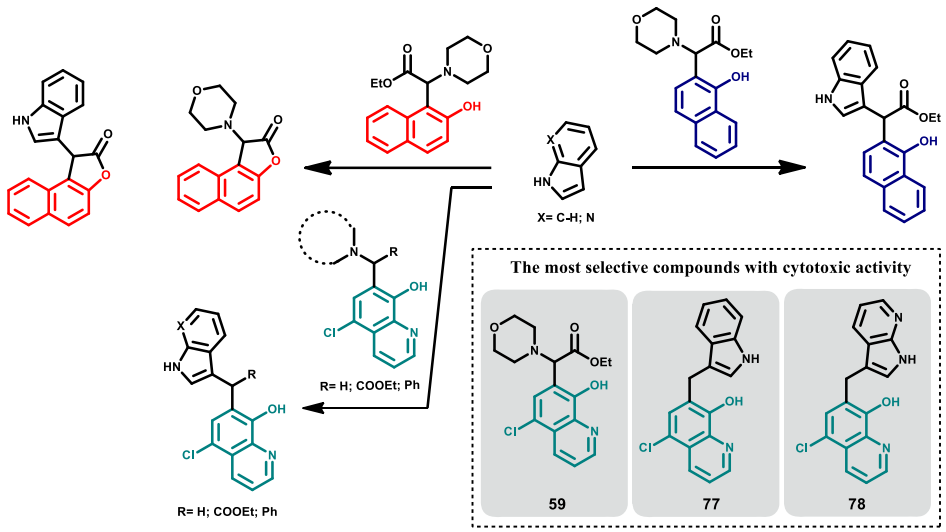

Figure 6. The most selective compounds with cytotoxic activity based on evaluations on sensitive (Colo205) and resistant (Colo320) colon adenocarcinoma and MRC-5 normal embryonal fibroblast cell lines.

considered selective, as they were not toxic to normal fibroblast cells (Table 10). Doxorubicin was applied as a positive control, and DMSO was the solvent control. In our research, the selectivity of the compounds toward cancer cells (when the activity is compared to normal cells) was investigated. The potential collateral selectivity of the derivatives was also tested applying sensitive Colo 205 colon adenocarcinoma cells and ABCB1 and LRP expressing resistant Colo 320 cells.[101] Relative resistance (RR) values were calculated as the ratio between the IC_{50} of a compound against the resistant cells and the IC_{50} against the corresponding sensitive cells (**Table 11**). Compounds with RR < 1 show selectivity against resistant cells, whereas RR ≤ 0.5 means that the compounds are highly selective towards resistant cells. All derivatives, with the exception of **75**, were selective toward resistant tumor cells. Furthermore, **77** exerted high potency to eliminate the MDR Colo320 cells (RR = 0.37), and this derivative showed no toxicity on normal MRC-5 cells being the most powerful scaffold in the series (**Figure 6**).

5. Summary and Outlook

Novel bifunctional precursors substituted with 2- and 1-naphthol or 5-chloro-8-hydroxyquinoline were synthesized by the reaction of 2- and 1-naphthol or 5-chloro-8-hydroxyquinoline, morpholine, and ethyl glyoxylate as the aldehyde component by using a modified Mannich-type synthetic pathway. The stabilization of Mannich bases via partially aromatic *ortho*-quinone methide intermediate was tested with different cyclic imines in [4 + 2] cycloaddition. Glycine derivatives bearing 2-, and 1-naphthol were reacted with indole and 7-azaindole. Reactions were found to depend on the naphthol skeleton. Starting from the 2-naphthol-substituted precursor, lactam-type ring-closed products were isolated. The transformation of 1-naphthol, in turn, led to the formation of the desired biaryl ester. The formed Mannich base substituted with 5-chloro-8-hydroxyquinoline was subjected to give diarylmethane derivatives with indole and 7-azaindole. The effect of the aldehyde component and the amine part of the Mannich base on the synthetic pathway was also investigated. A series of cyclic amines coupled with indole and azaindole derivatives has been systematically designed. The investigated precursors were synthesized by the coupling of indole with different cyclic imines. By fixing the isoquinoline part, the influence of the indole skeleton was also varied among indole-2-carboxylic acid, 4-, 5-, 6-, and 7-azaindoles. To have a comprehensive analysis about the correlation between structure and biological activity, the 7-azaindole analogs of the previously mentioned C-3-substituted indoles were also resynthesized or synthesized by using the modified *aza*-Friedel–Crafts reaction. The preparation of new 7-azaindole derivatives starting from 6,7-dimethoxy-3,4-dihydroisoquinoline as cyclic imine and (4*aR*,8*aR*)-4*a*,5,6,7,8,8*a*-hexahydroquinoxalin-2(1*H*)-one as chiral cyclic imine was also achieved by using MW conditions. In favor of having a preliminary overview about the structure–activity relationships, our efforts were focused on having an overview about biological activity of synthesized compounds by preliminary biological screening systems.

Acknowledgements

The authors thank the Hungarian Research Foundation (OTKA No. K-138871), the Ministry of Human Capacities,

Hungary grant, TKP-2021-EGA-32. N.S. was supported by the ÚNKP-23-4-SZTE-347 New National Excellence Program of the Ministry for Innovation and Technology from the source of the National Research, Development and Innovation Fund. G.S. was supported by the János Bolyai Research Scholarship (BO/00158/22/5) of the Hungarian Academy of Sciences and by the ÚNKP-23-5-SZTE-677 New National Excellence Program of the Ministry for Culture and Innovation from the source of the National Research, Development and Innovation Fund.

Conflict of Interest

The authors declare no conflict of interest.

Data Availability Statement

The data that support the findings of this study are available from the corresponding author upon reasonable request.

References

[1] S. K. Bur, S. F. Martin, *Tetrahedron* **2001**, *57*, 3221.
[2] W. N. Speckamp, M. J. Moolenaar, *Tetrahedron* **2000**, *56*, 3817.
[3] X. Lian, L. Lin, K. Fu, B. Ma, X. Liu, X. Feng, *Chem. Sci.* **2017**, *8*, 1238.
[4] S. Liras, J. E. Davoren, J. Bordner, *Org. Lett.* **2001**, *3*, 703.
[5] M. Ito, C. W. Clark, M. Mortimore, J. B. Goh, S. F. Martin, *J. Am. Chem. Soc.* **2001**, *123*, 8003.
[6] I. Szatmári, F. Fülöp, *Curr. Org. Synth.* **2004**, *1*, 155.
[7] V. F. S. Pape, R. Palkó, S. Tóth, M. J. Szabó, J. Sessler, G. Dormán, É.A. Enyedy, T. Soós, I. Szatmári, G. Szakács, *J. Med. Chem.* **2022**, *65*, 7729.
[8] I. Szatmári, F. Fülöp, *Tetrahedron Lett.* **2011**, *52*, 4440.
[9] I. Szatmári, M. Heydenreich, A. Koch, F. Fülöp, E. Kleinpeter, *Tetrahedron* **2013**, *69*, 7455.
[10] I. Szatmári, P. Barta, A. Csámpai, F. Fülöp, *Tetrahedron* **2017**, *73*, 4790.
[11] I. Szatmári, P. Barta, G. Tóth, A. Balázs, J. Halász, F. Fülöp, *Eur. J. Org. Chem.* **2017**, *37*, 5537.
[12] P. Barta, F. Fülöp, I. Szatmári, *Beilstein J. Org. Chem.* **2018**, *14*, 560.
[13] I. Szatmári, K. Belasri, M. Heydenreich, A. Koch, E. Kleinpeter, F. Fülöp, *Chem. Open* **2019**, *8*, 961.
[14] K. Belasri, L. Topal, M. Heydenreich, A. Koch, E. Kleinpeter, F. Fülöp, I. Szatmári, *Molecules* **2020**, *25*, 2524.
[15] R. Gupta, V. Luxami, K. Paul, *Bioorg. Chem.* **2021**, *108*, 104633.
[16] J. Kos, C. F. Ku, I. Kapustikova, M. Oravec, H. Zhang, J. Jampilek, *ChemistrySelect* **2019**, *4*, 4582.
[17] O. Dömötör, V. F. S. Pape, N. V. May, G. Szakács, É.A. Enyedy, *Dalton Trans.* **2017**, *46*, 4382.
[18] A. Albert, A. Hampton, F. R. Selbie, R. D. Simon, *Br. J. Exp. Pathol.* **1954**, *35*, 75.
[19] S. Zhai, L. Yang, Q. C. Cui, Y. Sun, Q. P. Dou, B. Yan, *J. Biol. Inorg. Chem.* **2010**, *15*, 259.
[20] T. Pillaiyar, M. Köse, K. Sylvester, H. Weighardt, D. Thimm, G. Borges, I. Förster, I. Kügelgen, C. E. Müller, *J. Med. Chem.* **2017**, *60*, 3636.
[21] V. I. Kiselev, V. M. Drukh, E. L. Muyzhnek, I. N. Kuznetsov, O. I. Pchelintseva, M. A. Paltsev, *Exp. Oncol.* **2014**, *36*, 90.
[22] S. Safe, S. Papineni, S. Chintharlapalli, *Cancer Lett.* **2008**, *269*, 326.
[23] B. Lőrinczi, P. Simon, I. Szatmári, *Int. J. Mol. Sci.* **2022**, *23*, 7152.
[24] I. Szatmári, J. Sas, F. Fülöp, *Tetrahedron Lett.* **2013**, *54*, 5069.
[25] J. Sas, I. Szatmári, F. Fülöp, *Curr. Org. Synth.* **2016**, *13*, 611.
[26] K. Belasri, F. Fülöp, I. Szatmári, *Molecules* **2019**, *24*, 3578.
[27] S. Chasset, F. Chevreuil, B. Ledoussal, F. Le Strat, R. Benarous, **2012**, Patent Number WO2012140243.
[28] M. Bihani, P. P. Bora, G. Bez, H. Askari, *C. R. Chim.* **2013**, *16*, 419.
[29] W. Chen, Y. K. Kang, R. G. Wilde, D. Seidel, *Angew. Chem. Int. Ed.* **2014**, *53*, 5179.
[30] Y. Zhou, L. Liu, J. Dong, S. Yin **2018**, Patent Number CN108947948.
[31] C. Cimarelli, D. Fratoni, A. Mazzanti, G. Palmieri, *Tetrahedron: Asymmetry* **2011**, *22*, 591.
[32] O. S. Rani, M. A. Devi, *Pharmacologyonline* **2009**, *3*, 743.
[33] R. Varala, V. Kotra, M. M. Alam, N. R. Kumar, S. Ganapaty, S. R. Adapa, *Indian J. Chem.* **2008**, *47B*, 1243.
[34] M. Yamaye, H. Okano, Y. Motoyanagi, N. C. Toh, T. Yoshinaga, T. Tsuru, K. Mukae, *Synthesis* **2004**, *3*, 341.
[35] L. Feiler, T. Ruch, O. Wallquist, P. Nesvadba **2000**, Patent Number WO20000535A.
[36] J. G. Wilson, A. G. Katsifis, *Aust. J. Chem.* **2000**, *53*, 583.
[37] P. Grundmann, W. D. Fessner, *Adv. Synth. Catal.* **2008**, *350*, 1729.
[38] A. Olyaei, E. C. Parashkuhi, S. Raoufmoghaddam, M. Mahdieh Sadeghpour, *Synth. Commun.* **2010**, *40*, 3609.
[39] R. Csütörtöki, I. Szatmári, A. Mándi, T. Kurtán, F. Fülöp, *Synlett* **2011**, *13*, 1940.
[40] A. Citterio, M. Gandolfi, O. Piccolo, L. Filippini, L. Tinucci, E. Valoti, *Synthesis* **1984**, *9*, 760.
[41] T. Huang, C. J. Li, *Tetrahedron Lett.* **2000**, *41*, 6715.
[42] G. Szakacs, S. Toth, T. Soos, R. Ferenczi-Palko, A. Furedi, D. Turk, V. Pape, F. Fulop, I. Szatmari, G. Dorman **2017**, Patent Number HU2016000234.
[43] Y. Wan, Y. Li, C. Yan, M. Yan, Z. Tang, *Eur. J. Med. Chem.* **2019**, *183*, 111691.
[44] N. Meena, Bhawani, Sonam, K. Rangan, A. Kumar, *J. Org. Chem.* **2023**, *88*, 3022.
[45] M. N. Feofanov, B. A. Lozhkin, M. V. Anokhin, A. D. Averin, I. P. Beletskaya, *Mendeleev Commun.* **2018**, *28*, 429.
[46] Y. Hui, Q. Zhang, J. Jiang, L. Lin, X. Liu, X. Feng, *J. Org. Chem.* **2009**, *74*, 6878.
[47] H.-M. Dong, H.-H. Lu, L.-Q. Lu, C.-B. Chen, W.-J. Xiao, *Adv. Synth. Catal.* **2007**, *349*, 1597.
[48] J. Kang, Y. Gao, M. Zhang, X. Ding, Z. Wang, D. Ma, Q. Wang, *J. Agric. Food Chem.* **2020**, *68*, 7839.

[49] J. A. Rivas-Loaiza, C. E. Reyes-Escobedo, Y. Lopez, S. Rojas-Lima, J. P. García-Merinos, H. López-Ruiz, *Lett. Org. Chem.* **2019**, *16*, 959.
[50] X. Liu, S. Ma, P. H. Toy, *Org. Lett.* **2019**, *21*, 9212.
[51] B. L. Tornquist, G. de Paula Bueno, J. C. M. Willig, I. M. de Oliveira, H. A. Stefani, J. Rafique, S. Saba, B. A. Iglesias, G. V. Botteselle, F. Manarin, *ChemistrySelect* **2018**, *3*, 6358.
[52] J. P. G. Merinos, H. L. Ruíz, Y. López, S. R. Limaa, *Lett. Org. Chem.* **2015**, *12*, 332.
[53] R. Surasani, D. Kalita, K. B. Chandrasekhar, *Green Chem. Lett. Rev.* **2012**, *6*, 113.
[54] C. Huo, C. Sun, C. Wang, X. Jia, W. Wenju Chang, *ACS Sustainable Chem. Eng.* **2013**, *1*, 549.
[55] M. I. Dawson, M. Ye, X. Cao, L. Farhana, Q. Y. Hu, Y. Zhao, L. P. Xu, A. Kiselyuk, R. G. Correa, L. Yang, T. Hou, J. C. Reed, P. Itkin-Ansari, F. Levine, M. F. Sanner, J. A. Fontana, X. K. Zhanga, *ChemMedChem* **2009**, *4*, 1106.
[56] M. Soueidan, J. Collin, R. Gil, *Tetrahedron Lett.* **2006**, *47*, 5467.
[57] Z. Yin, Z. Wang, X. F. Wu, *Org. Biomol. Chem.* **2018**, *16*, 3707.
[58] Z. Nan, L. Yige, C. Zhili, Q. Wenling, *Synthesis* **2018**, *50*, 4063.
[59] X. H. Xu, A. Kusuda, E. Tokunaga, N. Shibata, *Green Chem.* **2011**, *13*, 46.
[60] L. Deng, H. Li **2007**, Patent Number WO2007064861 A2.
[61] J. Yang, F. Mei, S. Fu, Y. Gu, *Green Chem.* **2018**, *20*, 1367.
[62] Z. Li, B. Yu, *Chem. Eur. J.* **2019**, *25*, 16528.
[63] G. Desimoni, G. Faita, M. Mella, M. Toscanini, M. Boiocchi, *Eur. J. Org. Chem.* **2008**, *36*, 6232.
[64] Q. Kang, Z. A. Zhao, S. L. You, *Tetrahedron* **2009**, *65*, 1603.
[65] A. A. Amaral, J. C. M. Willig, C. F. A. Olguin, I. M. Oliveira, H. A. Stefani, G. V. Botteselled, F. Manarin, *J. Br. Chem. Soc.* **2023**, *34*, 1464.
[66] A. Janczuk, W. Zhang, W. Xie, S. Lou, J. P. Cheng, P. G. Wang, *Tetrahedron Lett.* **2002**, *43*, 4271.
[67] S. P. Roche, S. S. Samanta, M. M. J. Gosselina, *Chem. Commun.* **2014**, *50*, 2632.
[68] B. Jiang, Z. G. Huang, *Synthesis* **2005**, *13*, 2198.
[69] J. L. Zhao, L. Liu, H. B. Zhang, Y. C. Wu, D. Wang, Y. J. Chen, *Synlett* **2006**, *1*, 96.
[70] G. Desimoni, G. Faita, M. Mella, M. Toscanini, M. Boiocchi, *Eur. J. Org. Chem.* **2009**, *16*, 2627.
[71] Y. Bin, S. Yihui, Y. Shuo, Z. Huiqing, L. Zhonghua, L. Hui, **2021**, Patent Number CN113582906.
[72] D. Z. Lin, J. M. Huang, *Org. Lett.* **2019**, *21*, 5862.
[73] Y. Dong, X. Li, P. Ji, F. Gao, X. Meng, W. Wang, *Org. Lett.* **2022**, *24*, 5034.
[74] V. Dinesh, R. Nagarajan, *J. Org. Chem.* **2022**, *87*, 10359.
[75] V. Dinesh, R. Nagarajan, *Synlett* **2023**, *34*, 855.
[76] S. Mishra, R. Ghosh, *Indian J. Chem. Sect. B: Org. Chem. Incl. Med. Chem.* **2011**, *50B*, 1630.
[77] N. Azizi, L. Torkian, M. R. Saidi, *J. Mol. Catal. A: Chem.* **2007**, *275*, 109.
[78] S. Sato, T. Sato, *Carbohydr. Res.* **2005**, *340*, 2251.
[79] A. Wright, R. Mattern, R. S. Jacobs **2000**, Patent Number WO2000002857 A1.
[80] J. Chen, J. Tian, K. Wen, Q. Gao, J. Shi, X. Yao, T. Wu, X. Tang, *Org. Biomol. Chem.* **2022**, *20*, 1652.
[81] P. P. Sathieshkumar, M. D. A. Saibabu, R. Nagarajan, *J. Org. Chem.* **2021**, *86*, 3730.
[82] J. Markus, B. Ferko, D. Berkeš, J. Moncol, A. M. Lawson, M. Othman, A. Daïch, *Eur. J. Org. Chem.* **2019**, *2019*, 5662.
[83] M. Ghandi, A. Taheri, *Molecules* **2009**, *14*, 1056.
[84] A. Das, K. Watanabe, H. Morimoto, T. Ohshima, *Org. Lett.* **2017**, *19*, 5794.
[85] D. Naskar, S. Neogi, A. Roy, A. B. Mandal, *Tetrahedron Lett.* **2008**, *49*, 6762.
[86] D. Hegedűs, N. Szemerédi, G. Spengler, I. Szatmári, *Eur. J. Med. Chem.* **2022**, *237*, 114391.
[87] E. Biekert, T. Funck, *Chem. Ber.* **1964**, *97*, 363.
[88] B. Matuszczak, *Monatsh Chem.* **1997**, *128*, 945.
[89] D. Hegedűs, N. Szemerédi, K. Petrinca, R. Berkecz, G. Spengler, I. Szatmári, *Molecules* **2024**, *29*, 4176.
[90] W. Herz, L. Tsai, *J. Am. Chem. Soc.* **1955**, *77*, 3529.
[91] Z. Chen, G. Hu, D. Li, J. Chen, Y. Li, H. Zhou, Y. Xie, *Bioorg. Med. Chem.* **2009**, *17*, 2351.
[92] S. Puri, K. Stefan, S. L. Khan, J. Pahnke, S. M. Stefan, K. Juvale, *J. Med. Chem.* **2023**, *66*, 657.
[93] S. D. Jadhav, A. Singh, *J. Org. Chem.* **2016**, *81*, 522.
[94] J. O. Liu, J. S. Shim, C. R. Chong, S. Bhat **2010**, Patent Number WO2010042163.
[95] J. P. Mészáros, J. M. Poljarević, I. Szatmári, O. Csuvik, F. Fülöp, N. Szoboszlai, G. Spengler, É.A. Enyedy, *Dalton Trans.* **2020**, *49*, 7977.
[96] G. W. Gribble, *Top. Heterocycl. Chem.*, Springer, Berlin, Heidelberg **2010**.
[97] D. Hegedűs, N. Szemerédi, M. Gábor, J. Sas, K. Belasri, I. Szatmári, G. Spengler, *Anticancer Res.* **2024**, *44*, 1149.
[98] J. Iwanejko, E. Wojaczyńska, J. Wojaczyński, J. Bąkowicz, *Tetrahedron Lett.* **2014**, *55*, 6619.
[99] T. Irie, M. Sawa, *Chem. Pharm. Bull.* **2018**, *66*, 29.
[100] G. Bollag, J. Tsai, J. Zhang, C. Zhang, P. Ibrahim, K. Nolop, P. Hirth, *Nature* **2012**, *11*, 873.
[101] S. A. R. Sancha, N. Szemerédi, G. Spengler, M. J. U. Ferreira, *Int. J. Mol. Sci.* **2023**, *24*, 2061.

Manuscript received: March 20, 2025
Revised manuscript received: April 16, 2025
Version of record online:

